Non-linear effects

Hannes BARTOSIK and Yannis PAPAPHILIPPOU
Accelerator and Beam Physics group
Beams Department
CERN

Joint University Accelerator School

Archamps, FRANCE

28-30 January 2015

Contents of the 2nd lecture

- Resonances and the path to chaos
  - Topology of 3rd and 4th order resonance
  - Path to chaos and resonance overlap
  - Dynamic aperture simulations
- Frequency map analysis
  - NAFF algorithm
  - Aspects of frequency maps
  - Frequency and diffusion maps for the LHC
  - Frequency map for lepton rings
  - Working point choice
  - Beam-beam effect
- Experiments
  - Experimental frequency maps
  - Beam loss frequency maps
  - Space-charge frequency scan

Contents of the 2nd lecture

- Resonances and the path to chaos
  - Topology of 3rd and 4th order resonance
  - Path to chaos and resonance overlap
  - Dynamic aperture simulations
- Frequency map analysis
  - NAFF algorithm
  - Aspects of frequency maps
  - Frequency and diffusion maps for the LHC
  - Frequency map for lepton rings
  - Working point choice
  - Beam-beam effect
- Experiments
  - Experimental frequency maps
  - Beam loss frequency maps
  - Space-charge frequency scan

Poincaré Section

- Record the particle coordinates at one location (BPM)
- Unperturbed motion lies on a circle in normalized coordinates (simple rotation)

Poincaré Section:

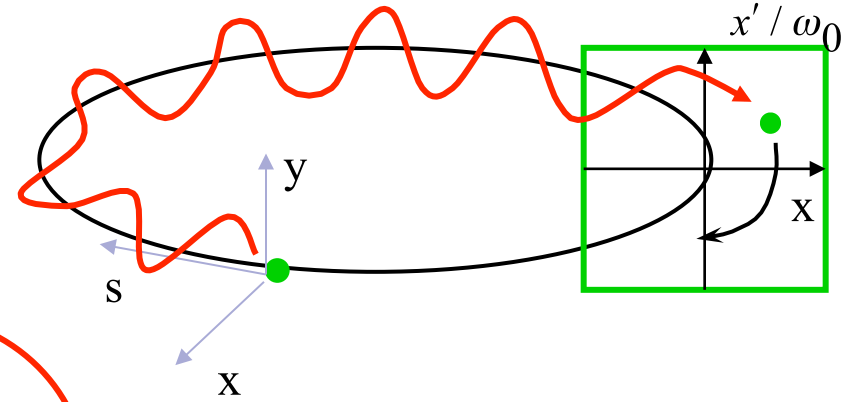

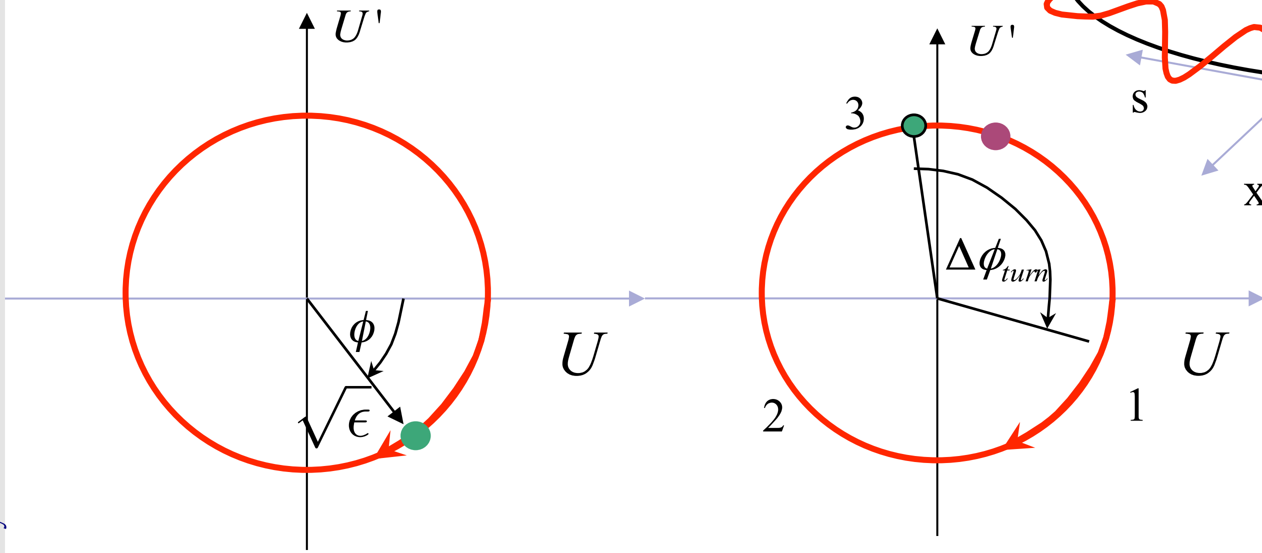

- Resonance condition corresponds to a periodic orbit or in fixed points in phase space
- For a sextupole $\delta\mathcal{U}' = \overline{b_3}\mathcal{U}^2$

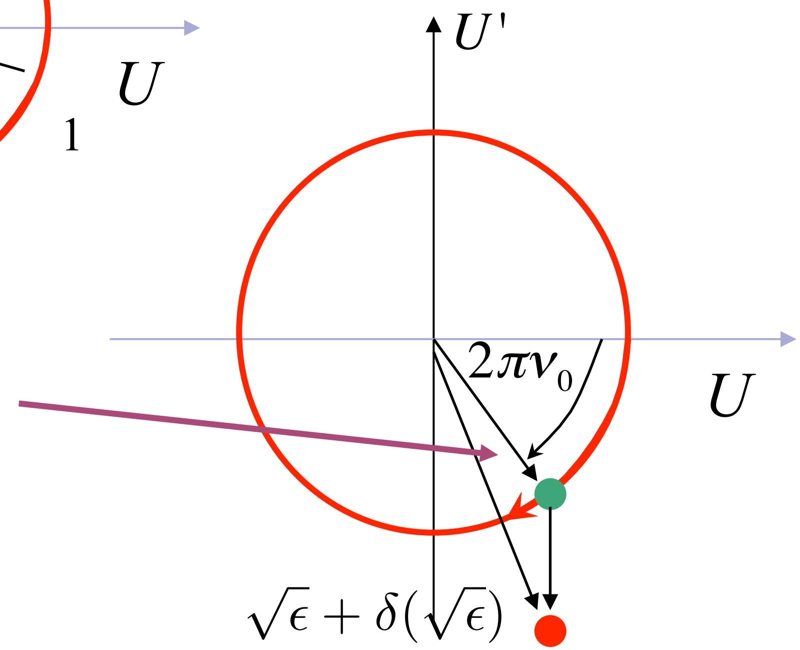

- The particle does not lie on a circle!

Fixed points for 3rd order resonance

- In the vicinity of a third order resonance, three fixed points can be found at $$\psi_{20} = \frac{\pi}{3}\,,\ \frac{3\pi}{3}\,,\ \frac{5\pi}{3}\,,\quad J_{20} = \left(\frac{2\delta}{3A_{3p}}\right)^2$$
- For $\frac{\delta}{A_{3p}} > 0$ all three points are unstable
- Close to the elliptic one at $\psi_{20} = 0$ the motion in phase space is described by circles that they get more and more distorted to end up in the "triangular" separatrix uniting the unstable fixed points

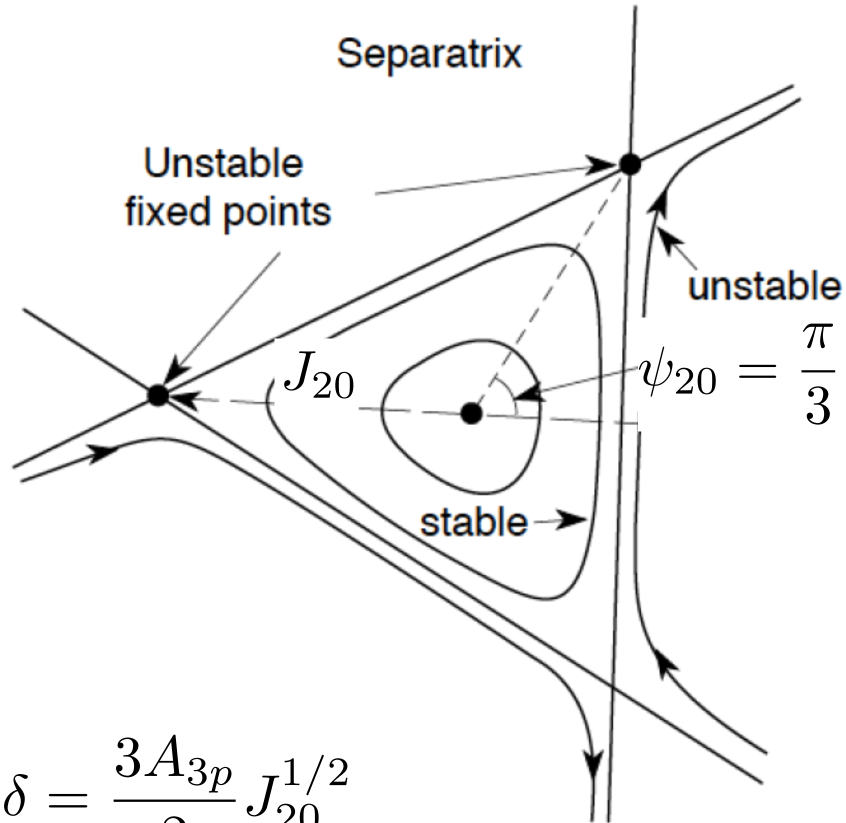

- The tune separation from the resonance (**stop-band width**) is $\delta = \frac{3A_{3p}}{2} J_{20}^{1/2}$

Topology of an octupole resonance

- Regular motion near the center, with curves getting more deformed towards a rectangular shape
- The separatrix passes through 4 unstable fixed points, but motion seems well contained
- Four stable fixed points exist and they are surrounded by stable motion (islands of stability)

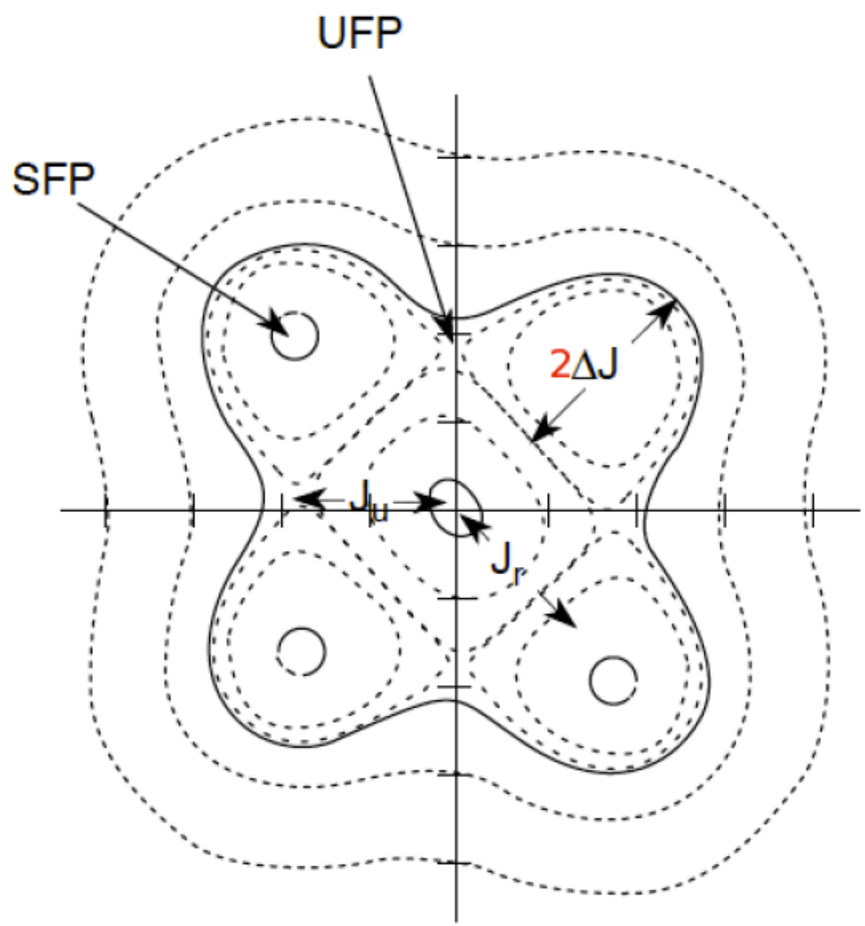

Path to chaos

- When perturbation becomes higher, motion around the separatrix becomes chaotic (producing tongues or splitting of the separatrix)
- Unstable fixed points are indeed the source of chaos when a perturbation is added

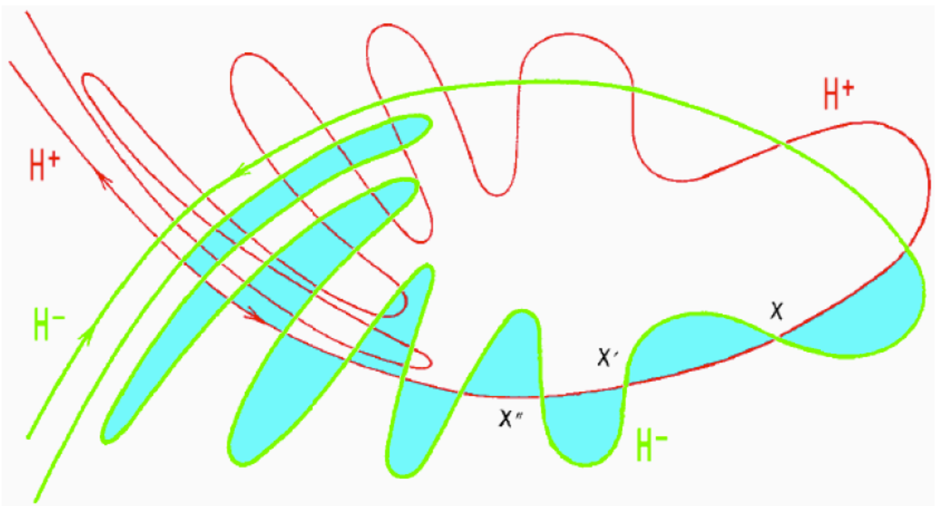

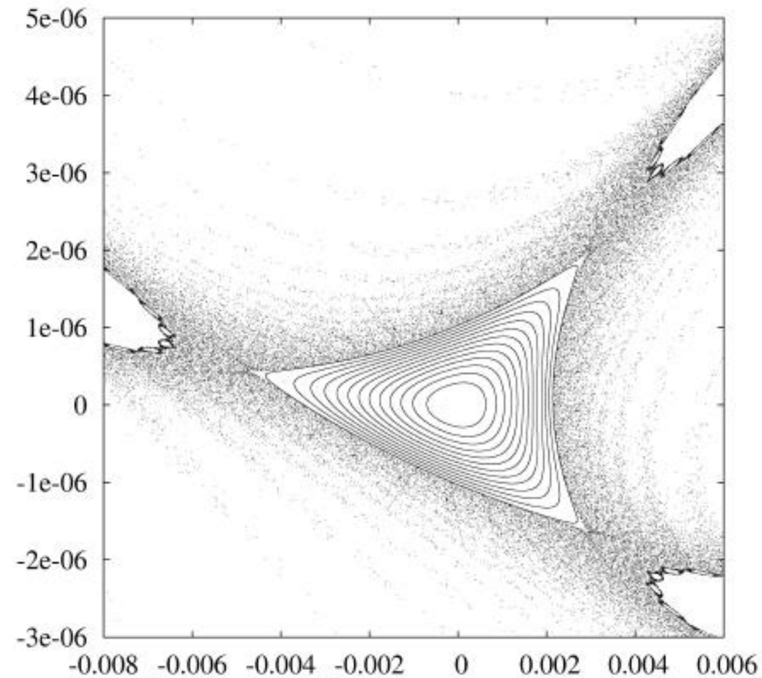

Chaotic motion

- Poincare-Birkhoff theorem states that under perturbation of a resonance only an even number of fixed points survives (half stable and the other half unstable)
- Themselves get destroyed when perturbation gets higher, etc. (self-similar fixed points)
- Resonance islands grow and resonances can overlap allowing diffusion of particles

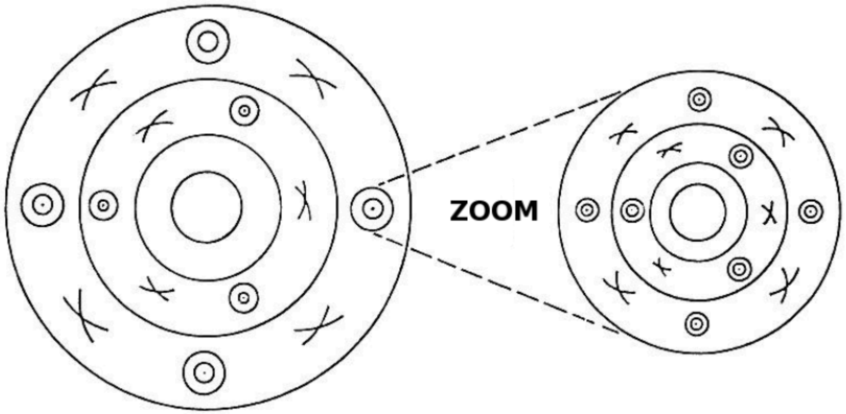

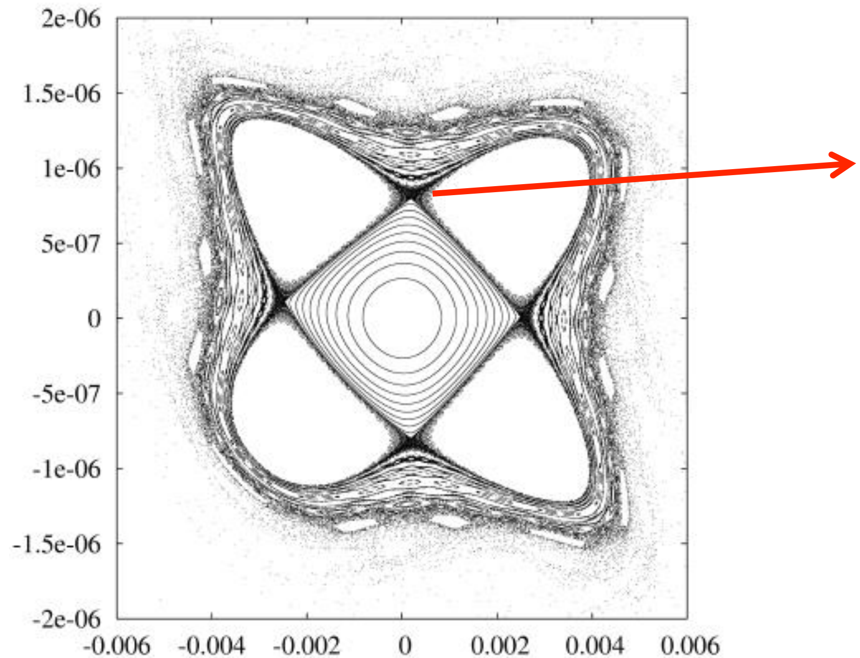

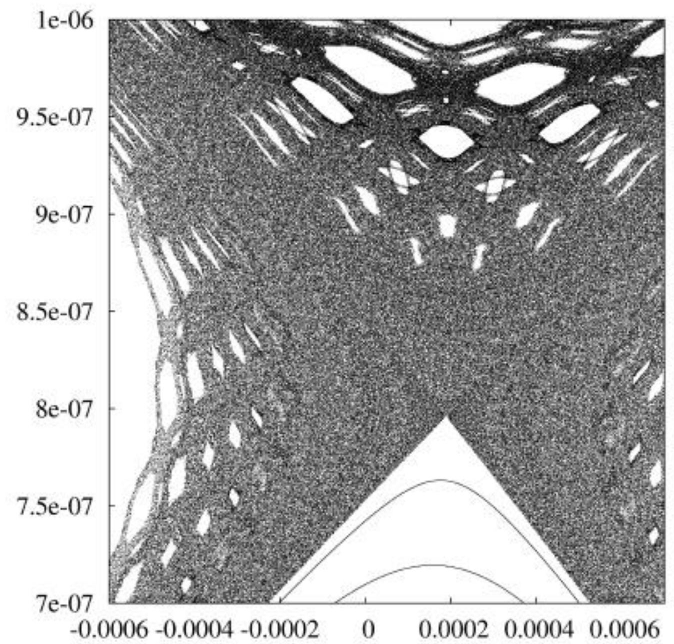

Resonance overlap criterion

- When perturbation grows, the resonance island width grows
- **Chirikov** (1960, 1979) proposed a criterion for the overlap of two neighboring resonances and the onset of orbit diffusion
- The distance between two resonances is $\delta\hat{J}_{1\ n,n'} = \dfrac{2\left(\frac{1}{n_1+n_2} - \frac{1}{n'_1+n'_2}\right)}{\left|\left.\frac{\partial^2 \bar{H}_0(\hat{\mathbf{J}})}{\partial \hat{J}_1^{\,2}}\right|_{\hat{J}_1=\hat{J}_{10}}\right|}$
- The simple overlap criterion is
  $$\Delta\hat{J}_{n\ max} + \Delta\hat{J}_{n'\ max} \geq \delta\hat{J}_{n,n'}$$
- Considering the width of chaotic layer and secondary islands, the "two thirds" rule apply $\Delta\hat{J}_{n\ max} + \Delta\hat{J}_{n'\ max} \geq \dfrac{2}{3}\delta\hat{J}_{n,n'}$
- The main limitation is the geometrical nature of the criterion (difficulty to be extended for > 2 degrees of freedom)

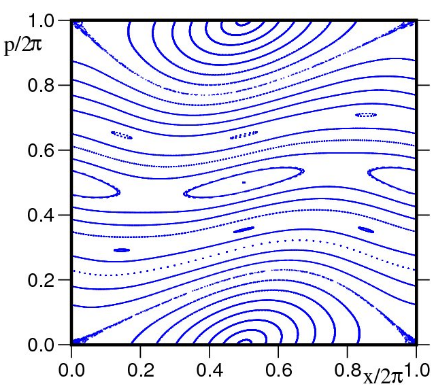

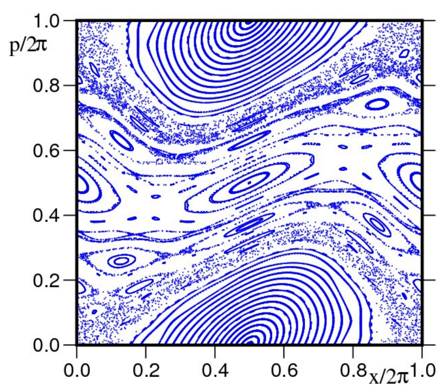

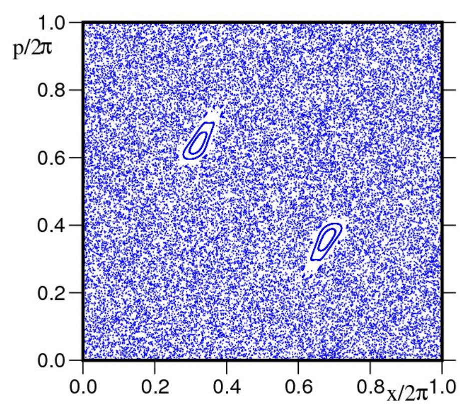

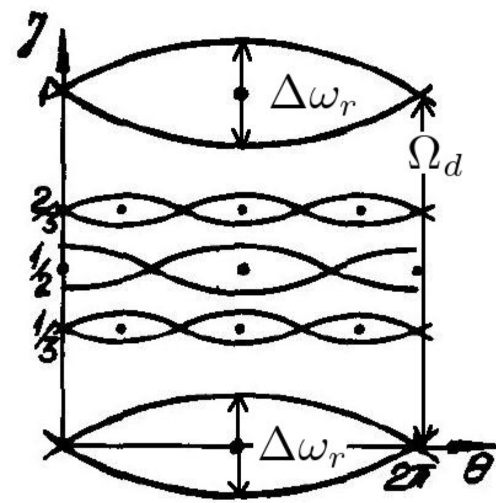

Beam Dynamics: Dynamic Aperture

- Dynamic aperture plots often show the maximum initial values of stable trajectories in x-y coordinate space at a particular point in the lattice, for a range of energy errors.
  - The beam size (injected or equilibrium) can be shown on the same plot.
  - Generally, the goal is to allow some significant margin in the design - the measured dynamic aperture is often significantly smaller than the predicted dynamic aperture.
- This is often useful for comparison, but is not a complete characterization of the dynamic aperture: a more thorough analysis is needed for full optimization.

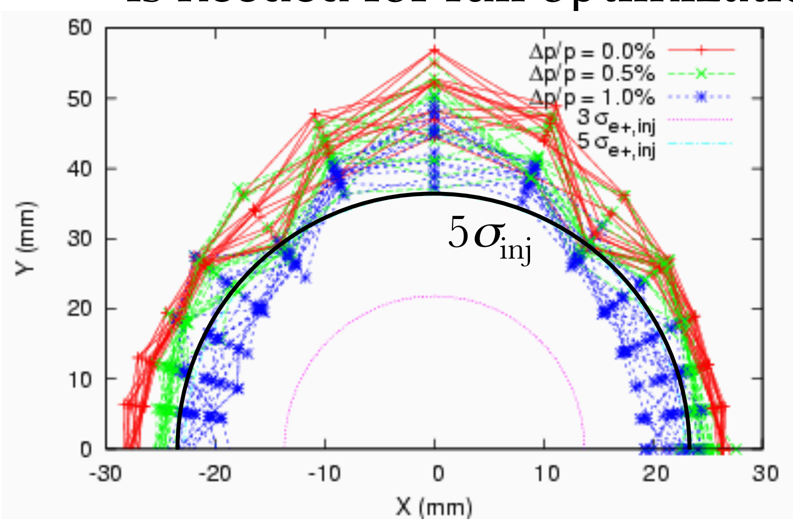

OCS: Circular TME

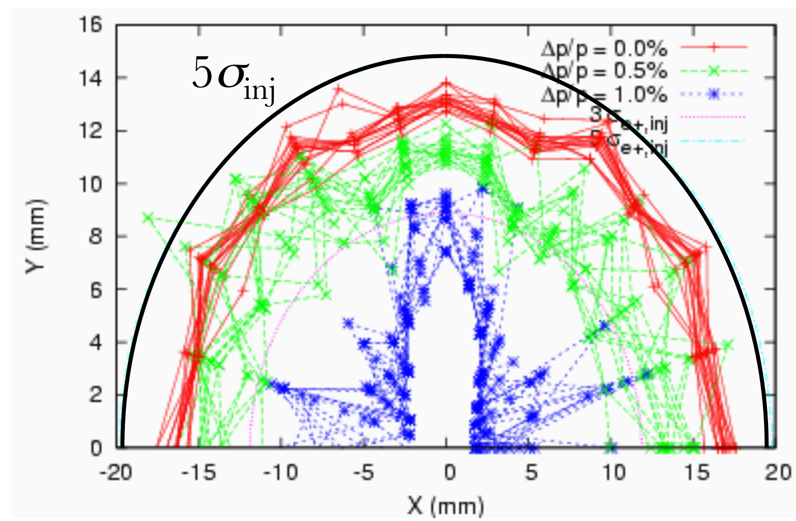

TESLA: Dogbone TME

Example: The ILC DR DA

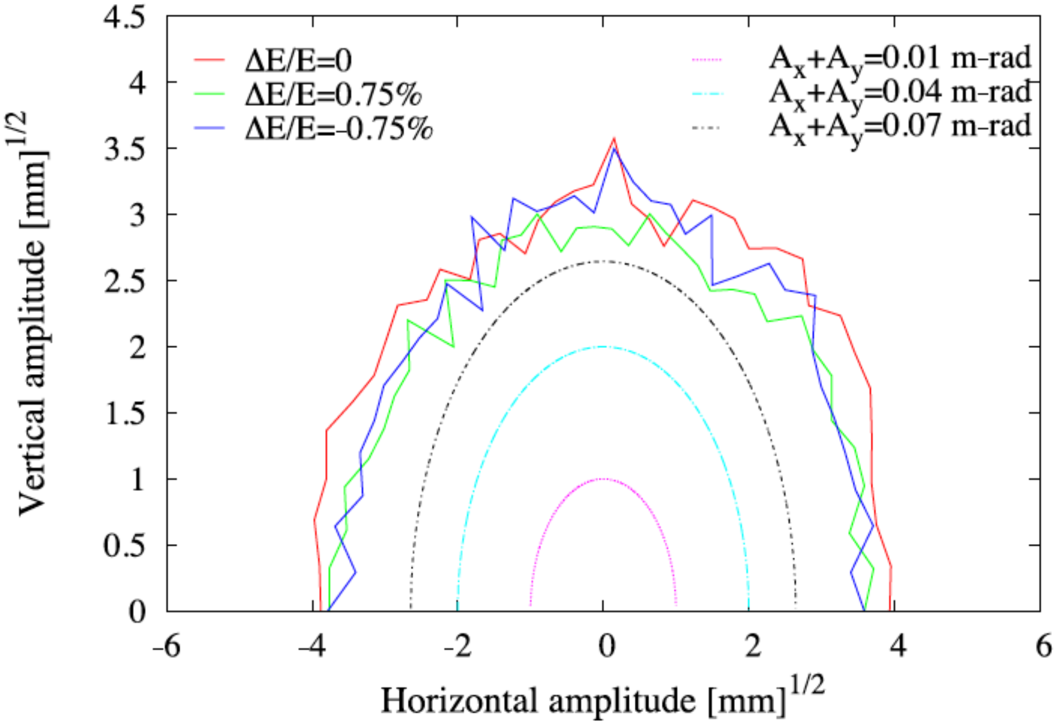

- Dynamic aperture for lattice with specified misalignments, multipole errors, and wiggler nonlinearities
- Specification for the phase space distribution of the injected positron bunch is an amplitude of **A**x + **A**y = 0.07m rad (normalized) and an energy spread of **E/E** 0.75%
- DA is larger then the specified beam acceptance

Dynamic aperture including damping

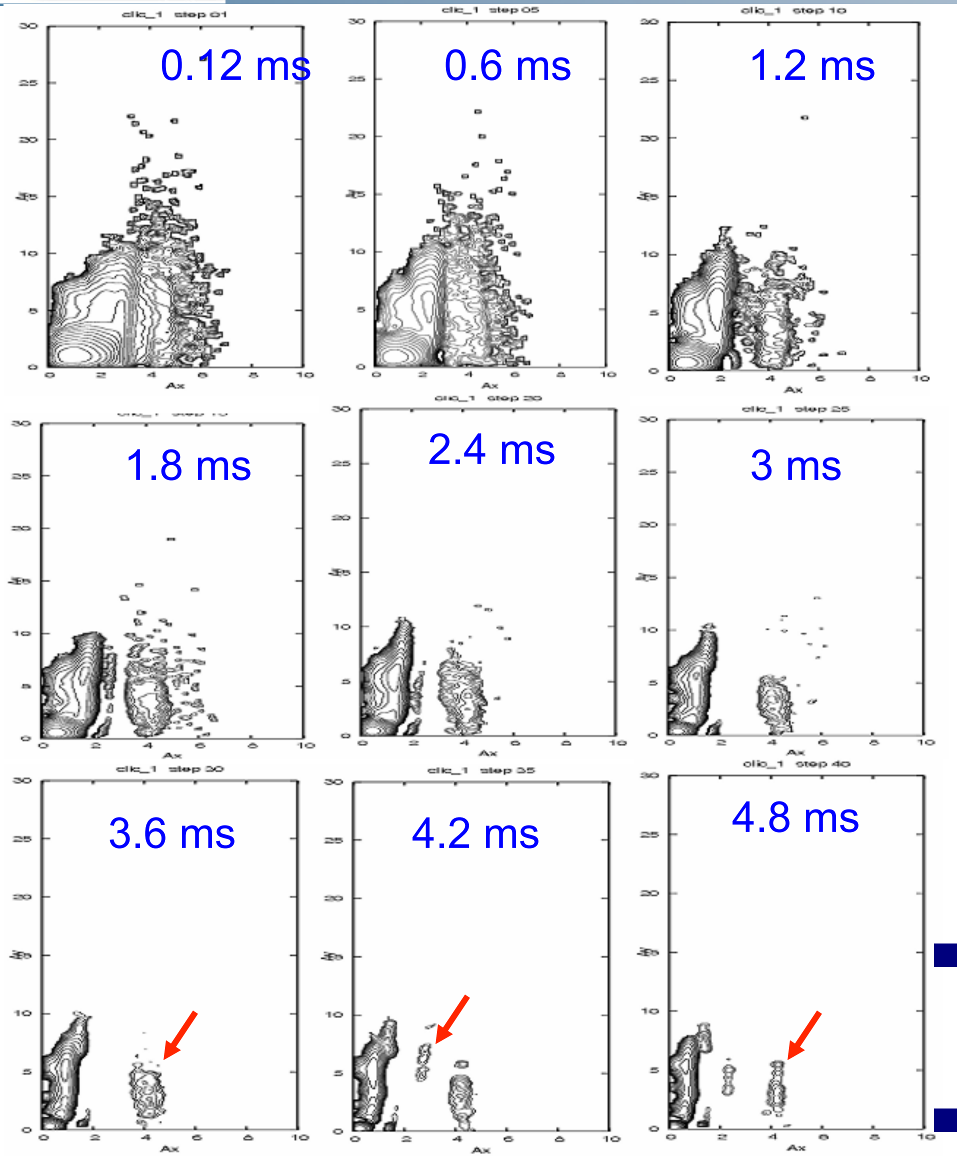

E. Levichev et al. PAC2009

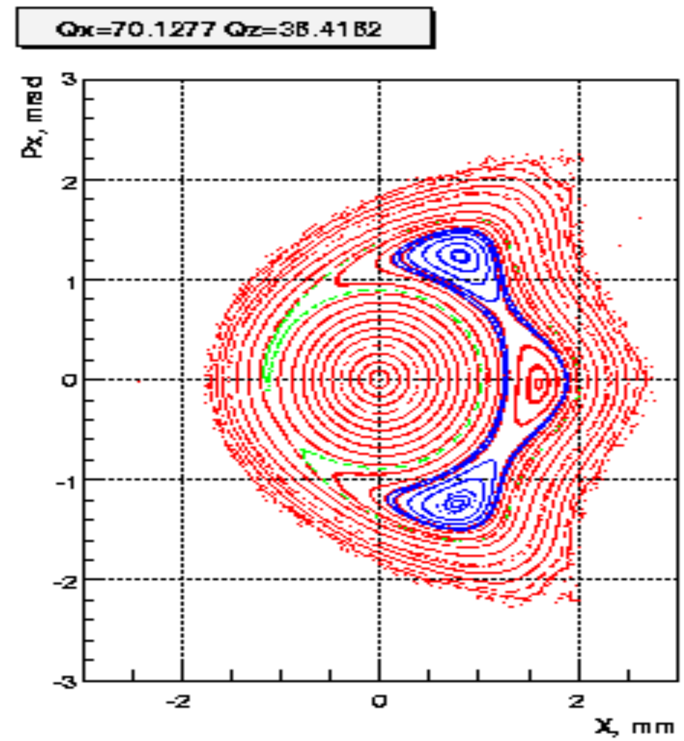

- Including radiation damping and excitation shows that 0.7% of the particles are lost during the damping
- Certain particles seem to damp away from the beam core, on resonance islands

Contents of the 2nd lecture

- Resonances and the path to chaos
  - Topology of 3rd and 4th order resonance
  - Path to chaos and resonance overlap
  - Dynamic aperture simulations
- Frequency map analysis
  - NAFF algorithm
  - Aspects of frequency maps
  - Frequency and diffusion maps for the LHC
  - Frequency map for lepton rings
  - Working point choice
  - Beam-beam effect
- Experiments
  - Experimental frequency maps
  - Beam loss frequency maps
  - Space-charge frequency scan

Frequency map analysis

- Frequency Map Analysis (FMA) is a numerical method which springs from the studies of J. Laskar (Paris Observatory) putting in evidence the chaotic motion in the Solar Systems
- FMA was successively applied to several dynamical systems
  - Stability of Earth Obliquity and climate stabilization (Laskar, Robutel, 1993)
  - 4D maps (Laskar 1993)
  - Galactic Dynamics (Y.P and Laskar, 1996 and 1998)
  - Accelerator beam dynamics: lepton and hadron rings (Dumas, Laskar, 1993, Laskar, Robin, 1996, Y.P, 1999, Nadolski and Laskar 2001)

NAFF algorithm

- When a quasi-periodic function $f(t) = q(t) + ip(t)$ in the complex domain is given numerically, it is possible to recover a quasi-periodic approximation

$$f'(t) = \sum_{k=1}^{N} a'_k e^{i\omega'_k t}$$

in a very precise way over a finite time span $[-T, T]$ several orders of magnitude more precisely than simple Fourier techniques

- This approximation is provided by the Numerical Analysis of Fundamental Frequencies – **NAFF** algorithm
- The frequencies ω'_k and complex amplitudes a'_k are computed through an iterative scheme.

Aspects of the frequency map

- In the vicinity of a resonance the system behaves like a pendulum
- Passing through the elliptic point for a fixed angle, a fixed frequency (or rotation number) is observed
- Passing through the hyperbolic point, a frequency jump is oberved

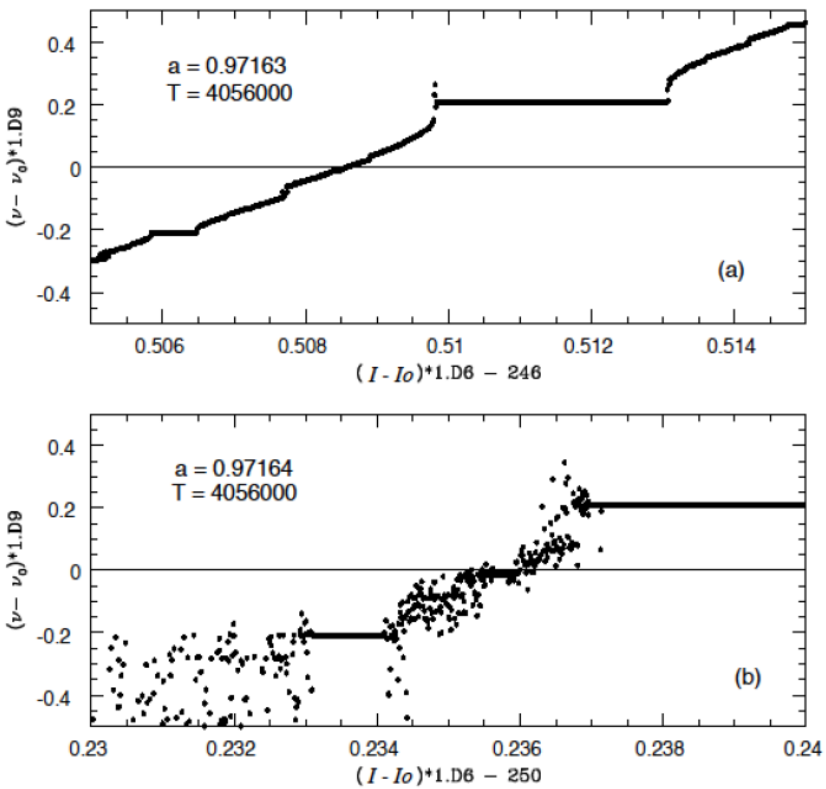

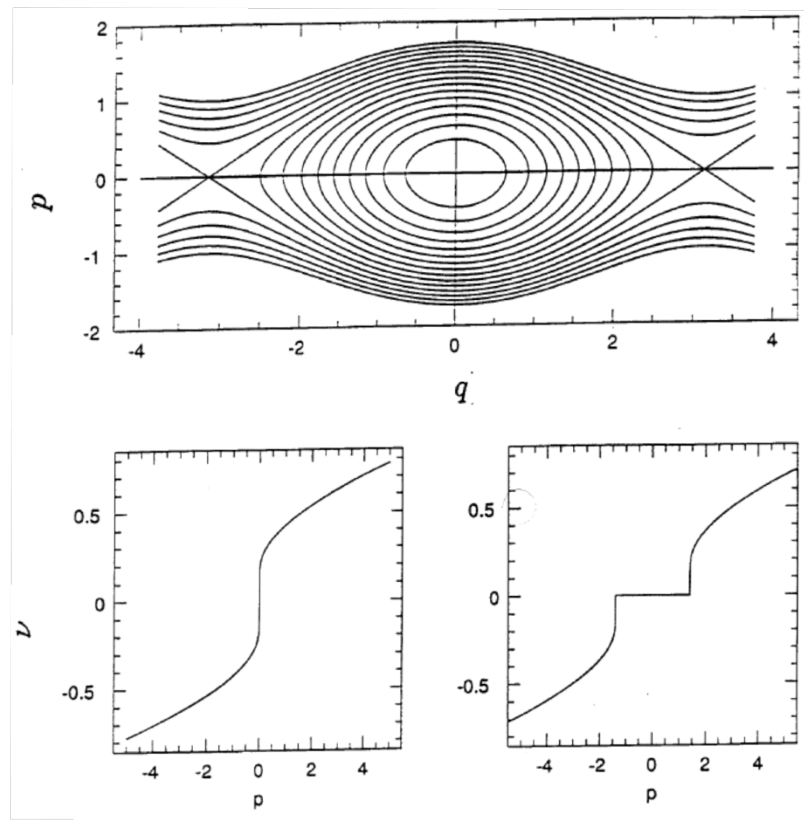

Building the frequency map

- Choose coordinates (x_i, y_i) with p_x and p_y=0
- Numerically integrate the phase trajectories through the lattice for sufficient number of turns
- Compute through NAFF Q_x and Q_y after sufficient number of turns
- Plot them in the tune diagram

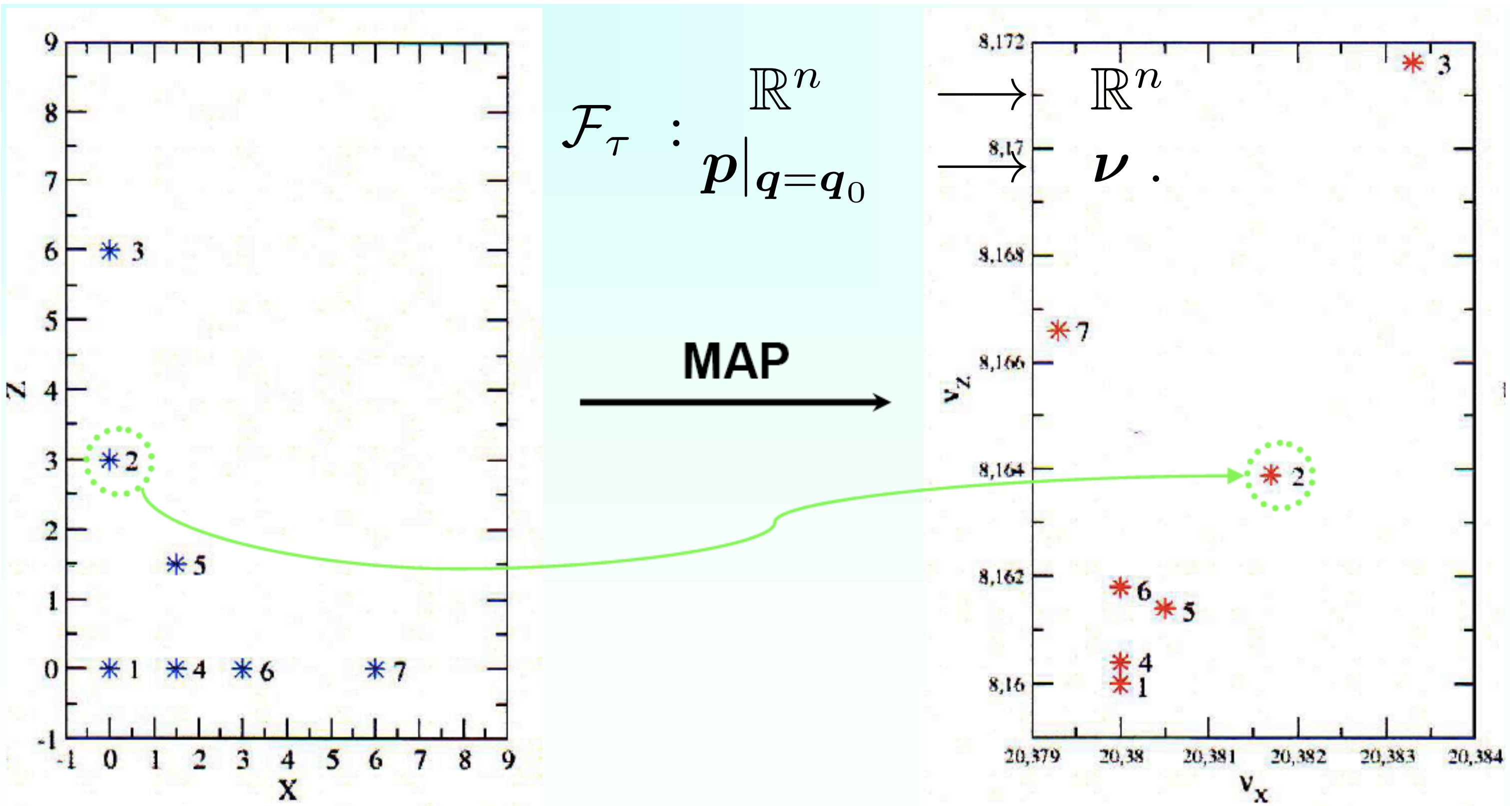

$$\mathcal{F}_\tau \; : \; \begin{array}{ccc} \mathbb{R}^n & \longrightarrow & \mathbb{R}^n \\ \boldsymbol{p}|_{\boldsymbol{q}=\boldsymbol{q}_0} & \longrightarrow & \boldsymbol{\nu} \end{array} .$$

Frequency maps for the LHC

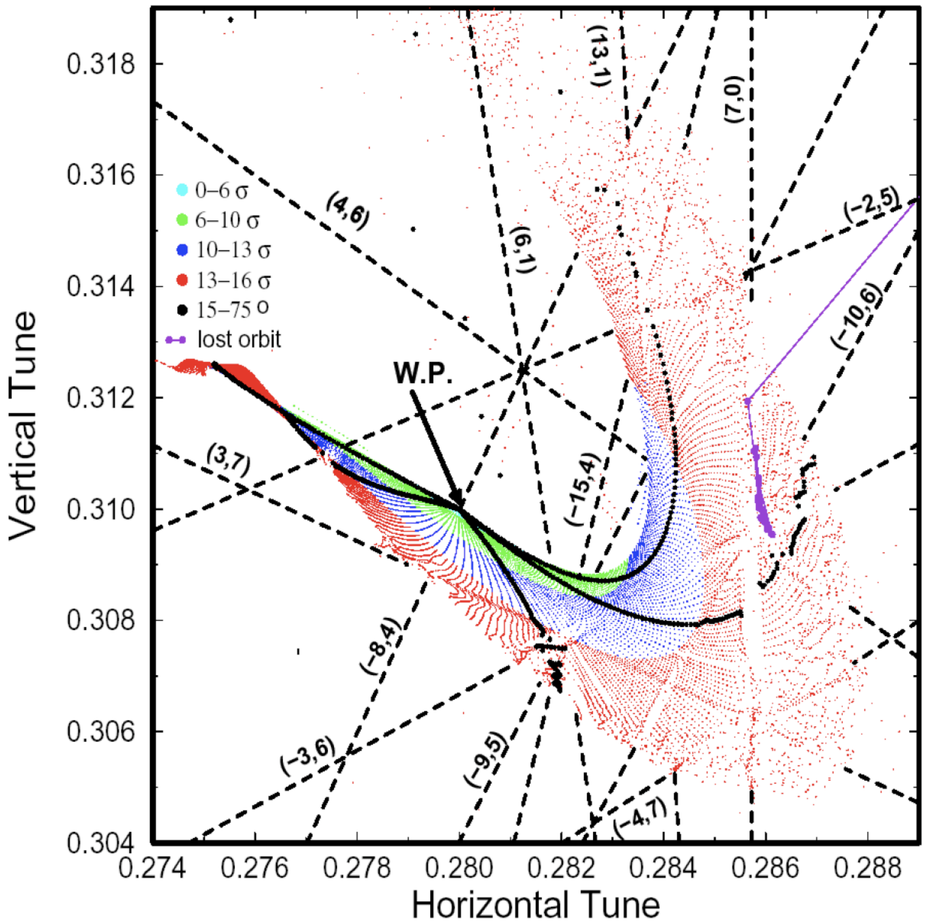

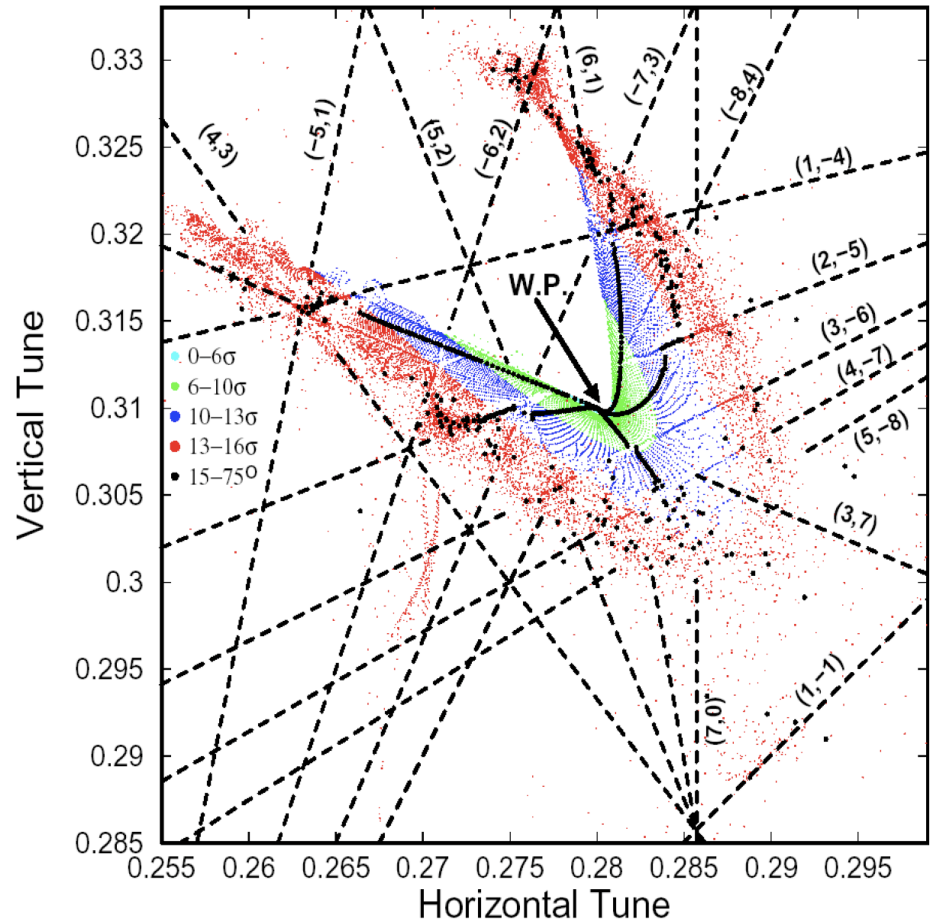

Frequency maps for the target error table (left) and an increased random skew octupole error in the super-conducting dipoles (right)

Diffusion Maps

J. Laskar, PhysicaD, 1993

- Calculate frequencies for two equal and successive time spans and compute frequency diffusion vector:

$$\boldsymbol{D}\big|_{t=\tau} = \boldsymbol{\nu}\big|_{t\in(0,\tau/2]} - \boldsymbol{\nu}\big|_{t\in(\tau/2,\tau]}$$

- Plot the initial condition space color-coded with the norm of the diffusion vector
- Compute a diffusion quality factor by averaging all diffusion coefficients normalized with the initial conditions radius

$$D_{QF} = \left\langle \frac{|\boldsymbol{D}|}{(I_{x0}^2 + I_{y0}^2)^{1/2}} \right\rangle_R$$

Diffusion maps for the LHC

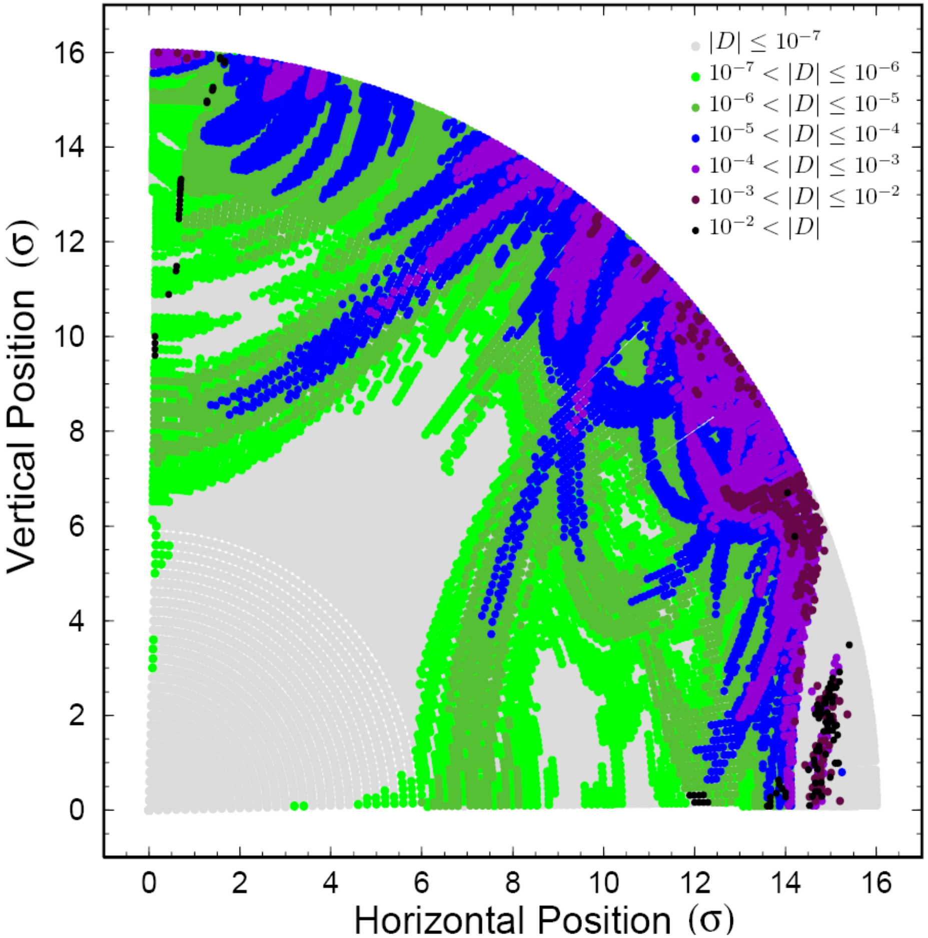

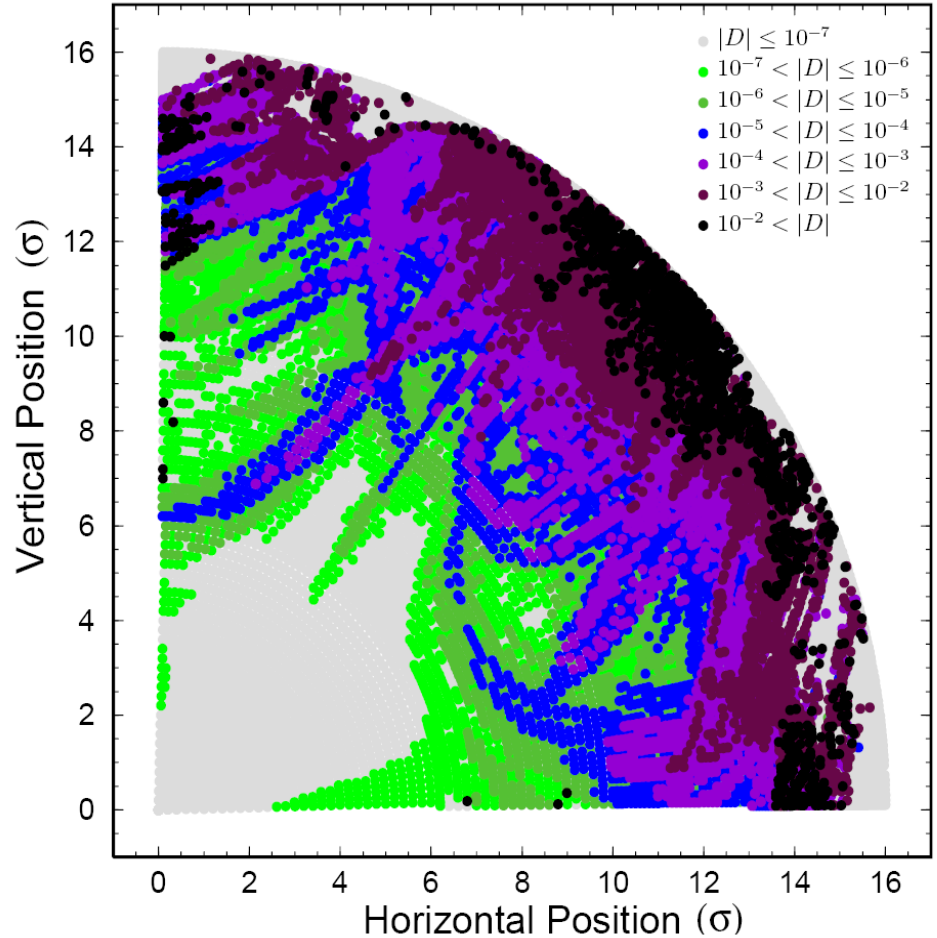

Diffusion maps for the target error table (left) and an increased random skew octupole error in the super-conducting dipoles (right)

Resonance free lattice for CLIC PDR

- Non linear optimization based on phase advance scan for minimization of resonance driving terms and tune-shift with amplitude

$$\left|\sum_{p=0}^{N_c-1} e^{ip(n_x\mu_{x,c}+n_y\mu_{y,c})}\right| = \sqrt{\frac{1-\cos\left[N_c(n_x\mu_{x,c}+n_y\mu_{y,c})\right]}{1-\cos(n_x\mu_{x,c}+n_y\mu_{y,c})}} = 0$$

$$\Downarrow$$

$$N_c(n_x\mu_{x,c}+n_y\mu_{y,c}) = 2k\pi$$

$$n_x\mu_{x,c}+n_y\mu_{y,c} \neq 2k'\pi$$

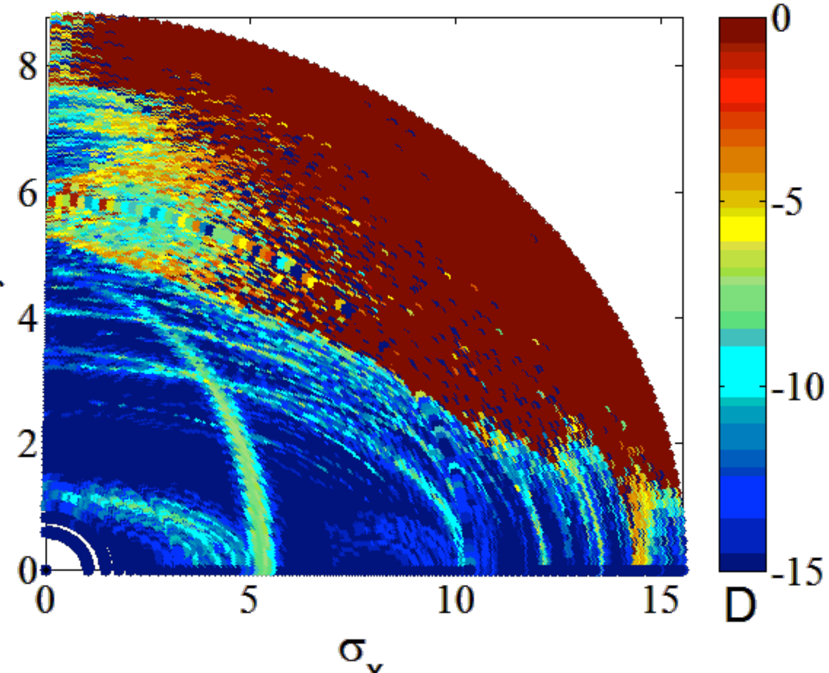

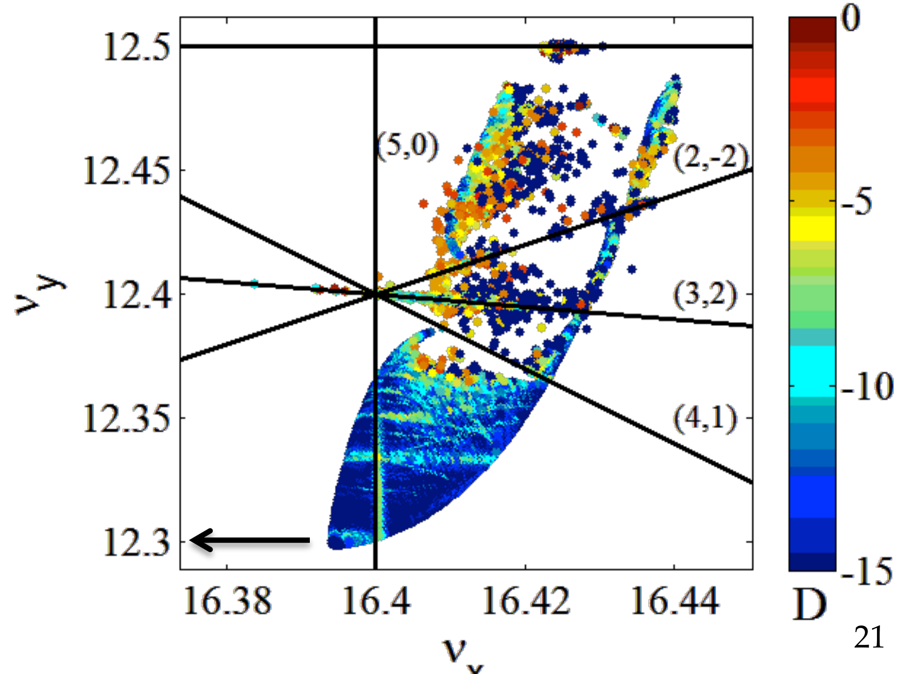

Dynamic aperture for CLIC DR

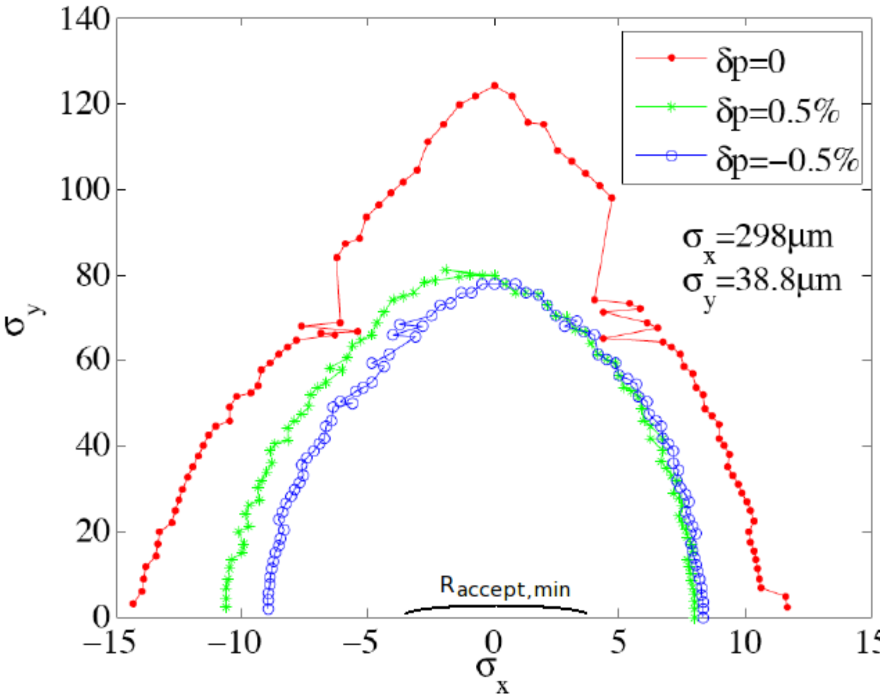

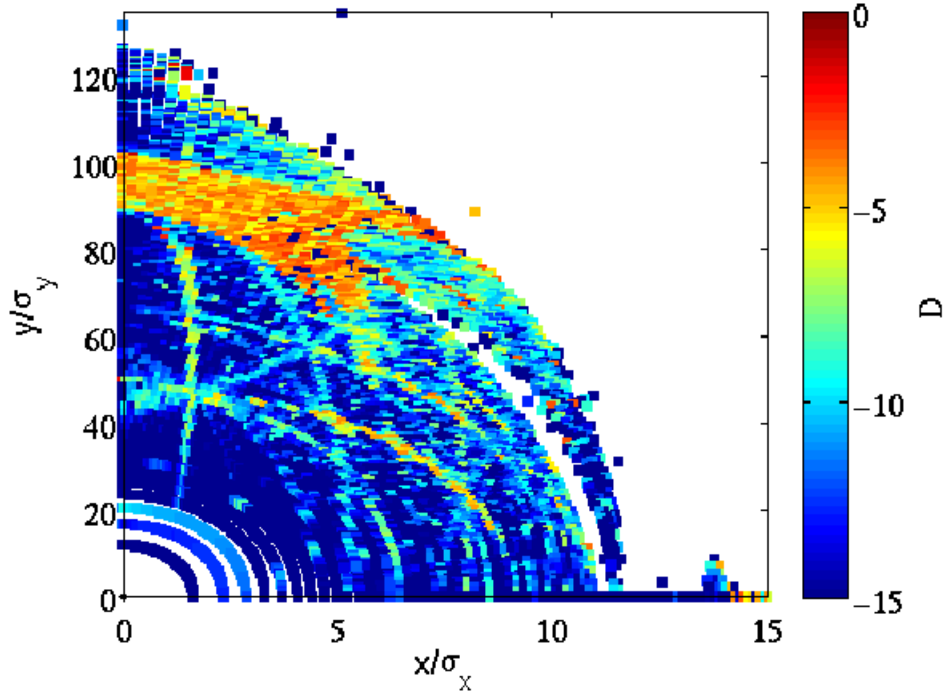

- Dynamic aperture and diffusion map
- Very comfortable DA especially in the vertical plane
  - Vertical beam size very small, to be reviewed especially for removing electron PDR
- Need to include non-linear fields of magnets and wigglers

Frequency maps for the ILC DR

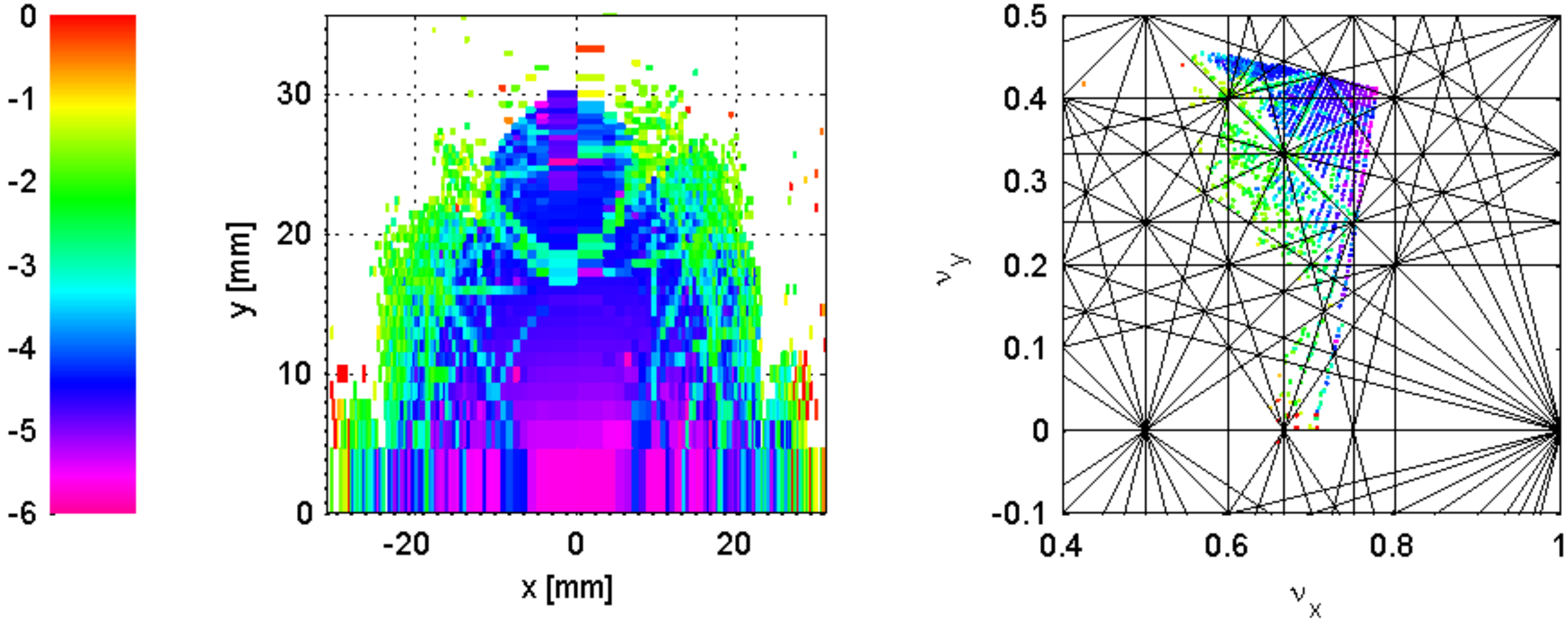

- Frequency maps enabled the comparison and steering of different lattice designs with respect to non-linear dynamics
  - Working point optimisation, on and off-momentum dynamics, effect of multi-pole errors in wigglers

- All dynamics represented in these two plots
- Regular motion represented by blue colors (close to zero amplitude particles or working point)

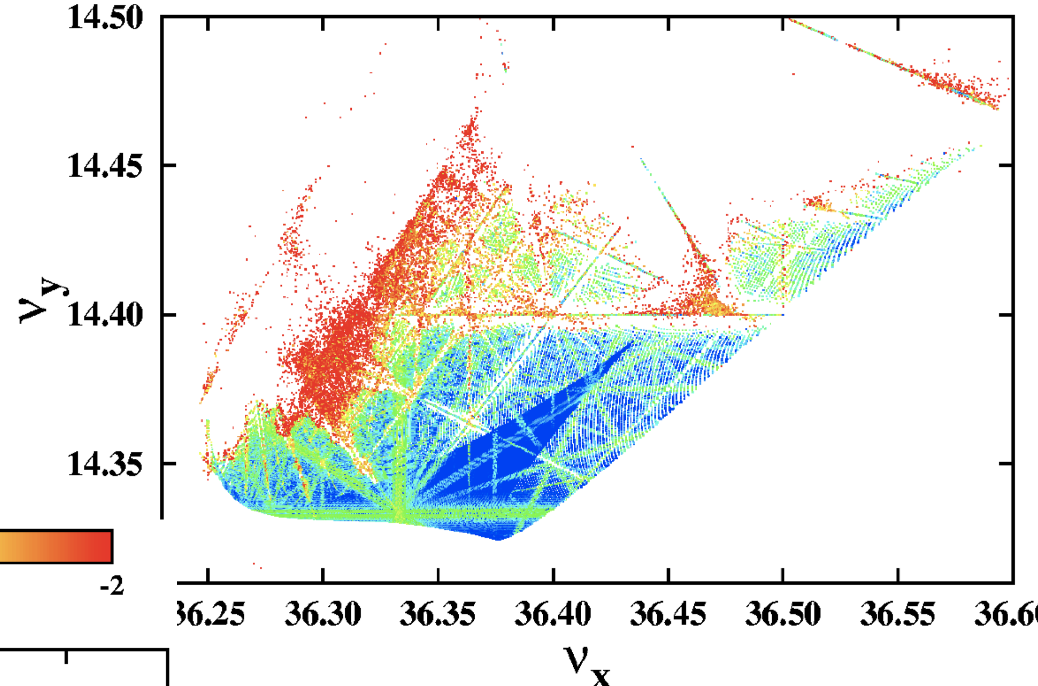

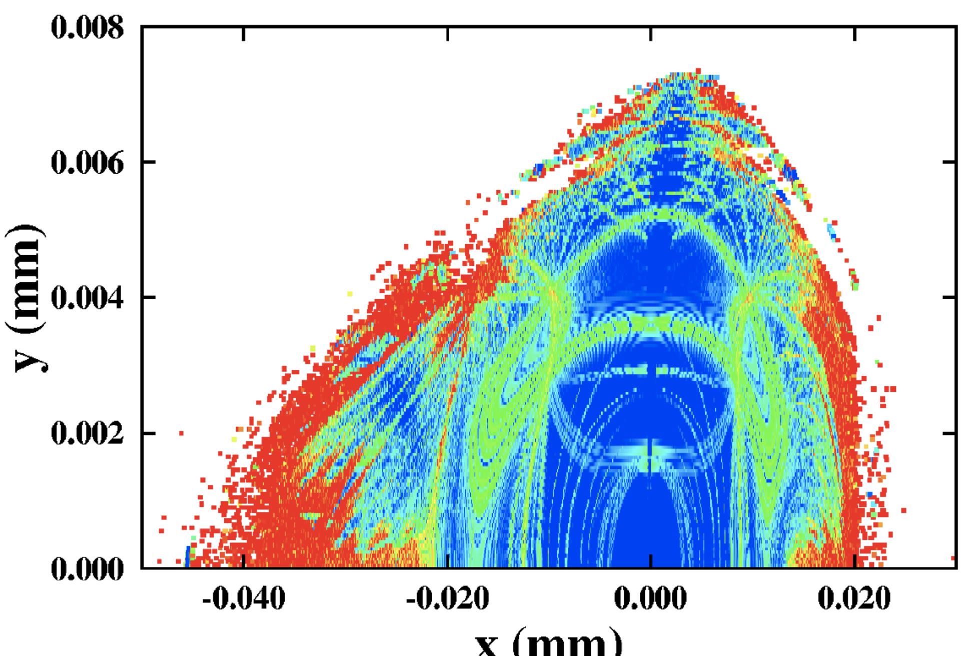

- Resonances appear as distorted lines in frequency space (or curves in initial condition space
- Chaotic motion is represented by red scattered particles and defines dynamic aperture of the machine

- Integrate a large number of particles
- Calculate the tune with refined Fourier analysis
- Plot points to tune space

$$\mathcal{F}_\tau \; : \; \begin{array}{ccc} \mathbb{R}^2 & \longrightarrow & \mathbb{R}^2 \\ (I_x, I_y)|_{p_x, p_y = 0}, & \longrightarrow & (\nu_x, \nu_y) \end{array}$$

SNS Working Point (Q_x,Q_y)=(6.4,6.3)

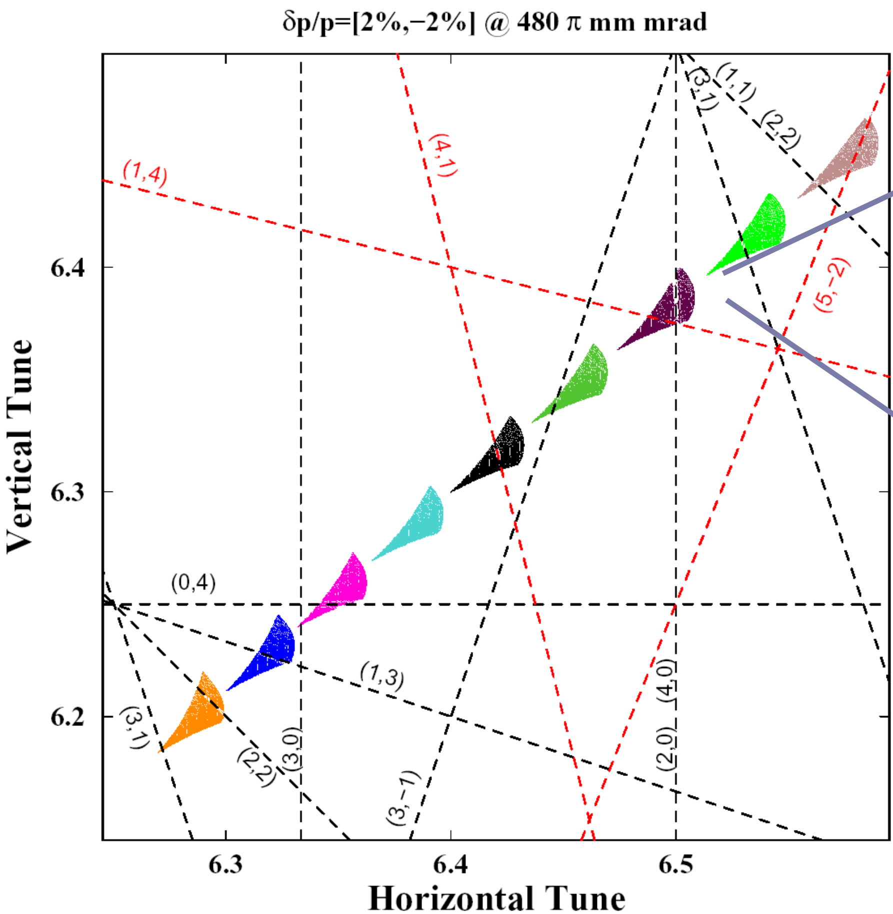

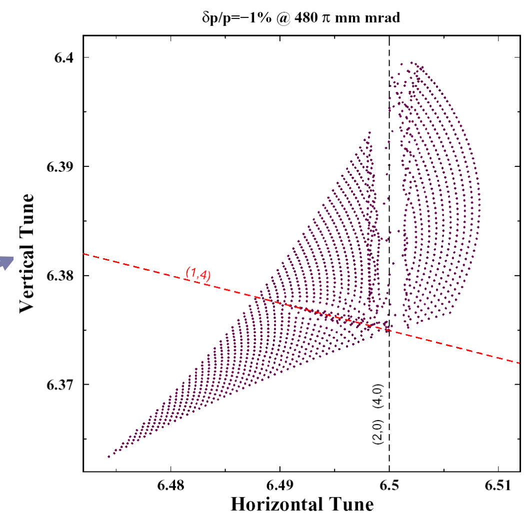

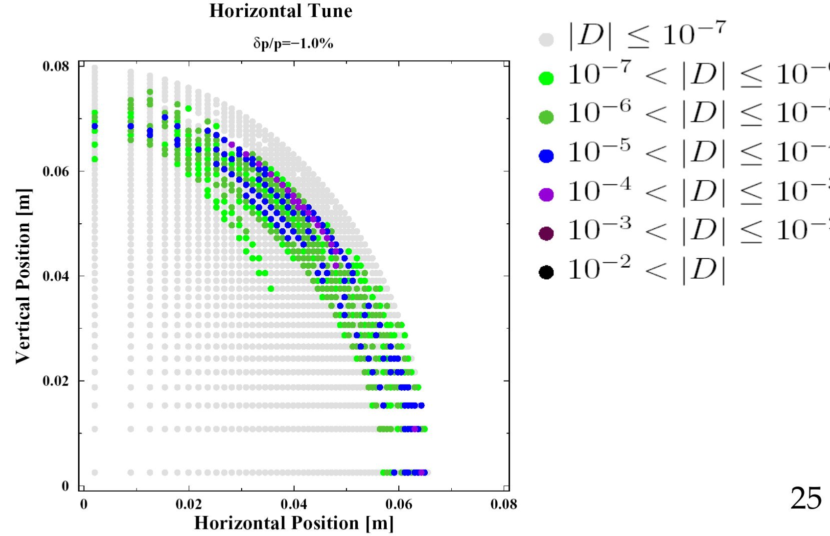

SNS Working point (6.23,5.24)

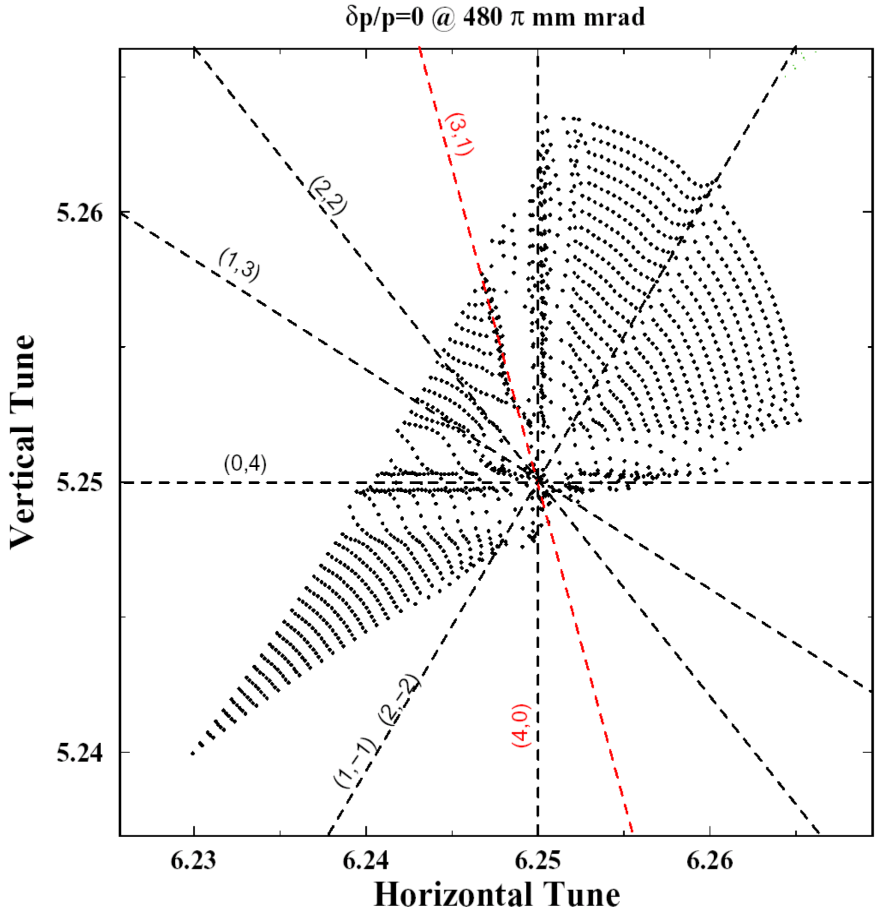

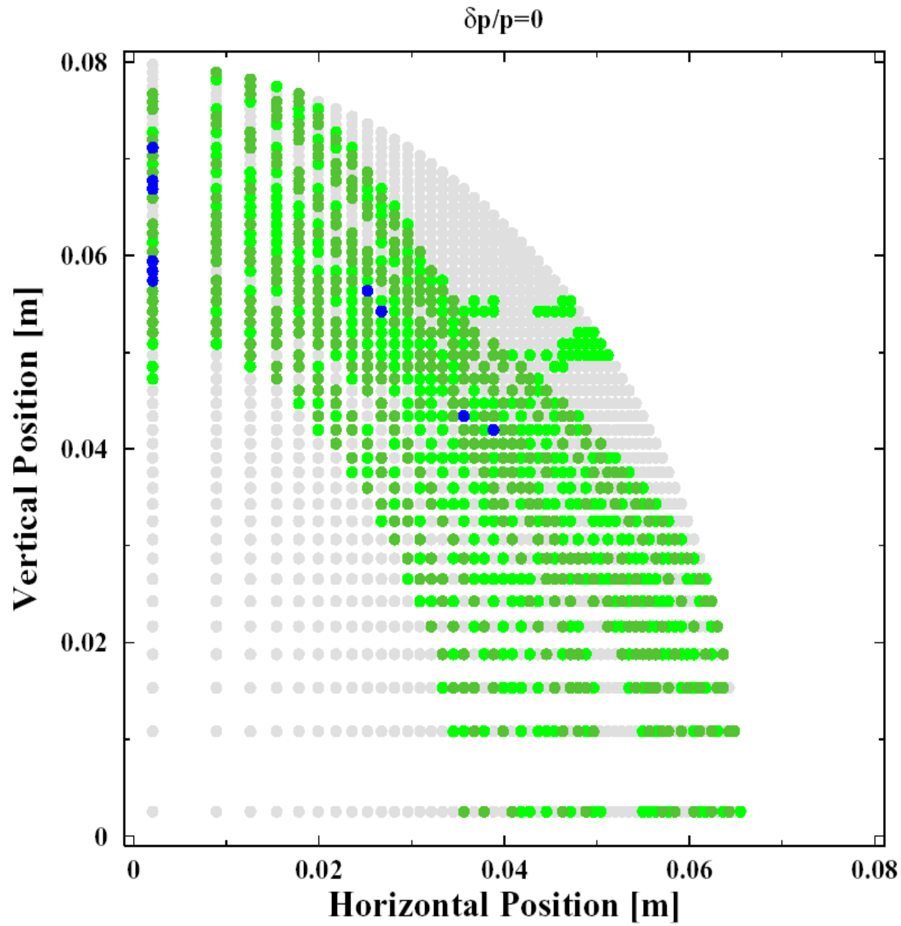

Tune Diffusion quality factor

$$D_{QF} = \left\langle \frac{|\boldsymbol{D}|}{(I_{x0}^2 + I_{y0}^2)^{1/2}} \right\rangle_R$$

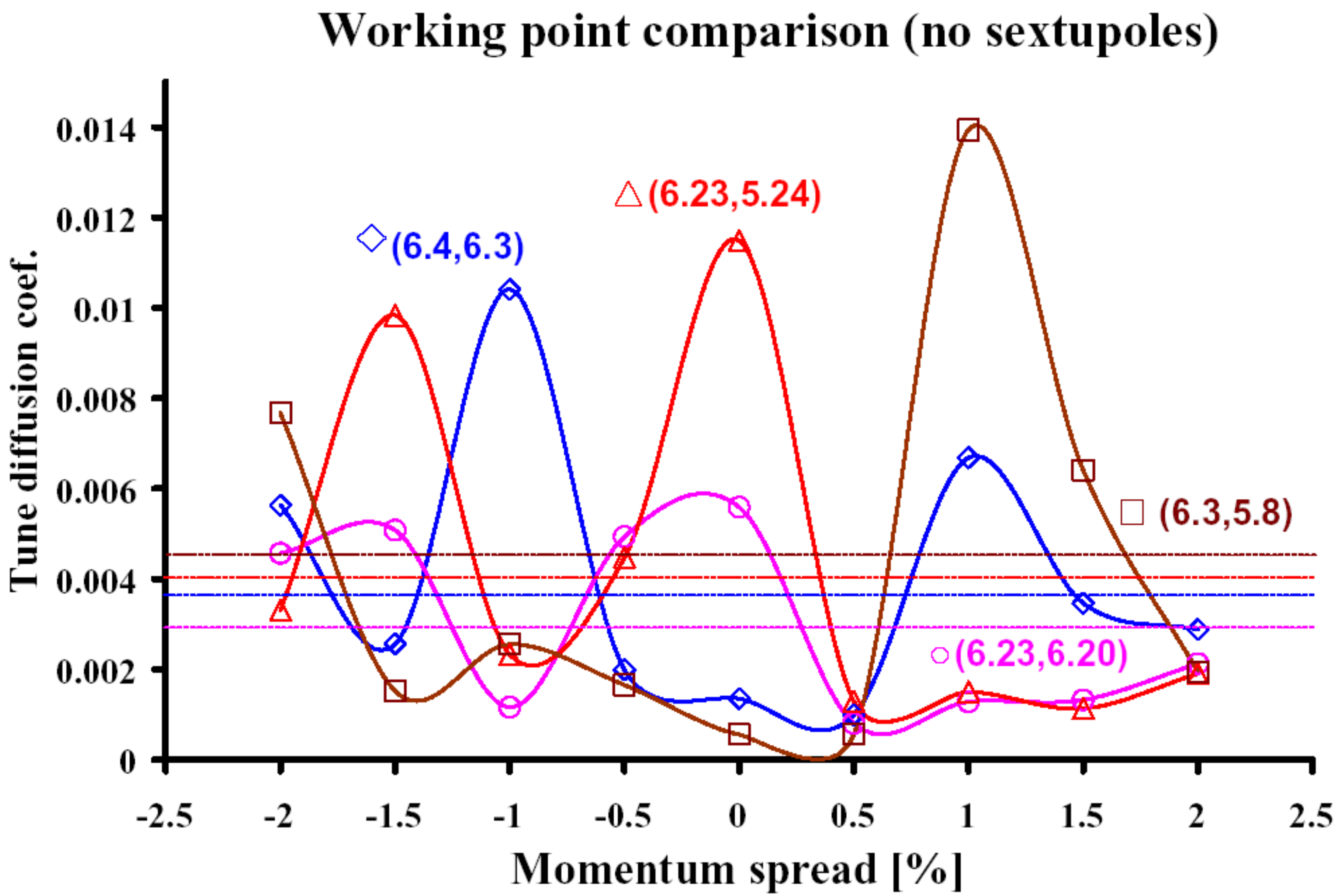

Working point choice for SUPERB

- Figure of merit for choosing best working point is sum of diffusion rates with a constant added for every lost particle
- Each point is produced after tracking 100 particles
- Nominal working point had to be moved towards "blue" area

$$e^D = \sqrt{\frac{(\nu_{x,1} - \nu_{x,2})^2 + (\nu_{y,1} - \nu_{y,2})^2}{N/2}}$$

S. Liuzzo et al., IPAC 2012

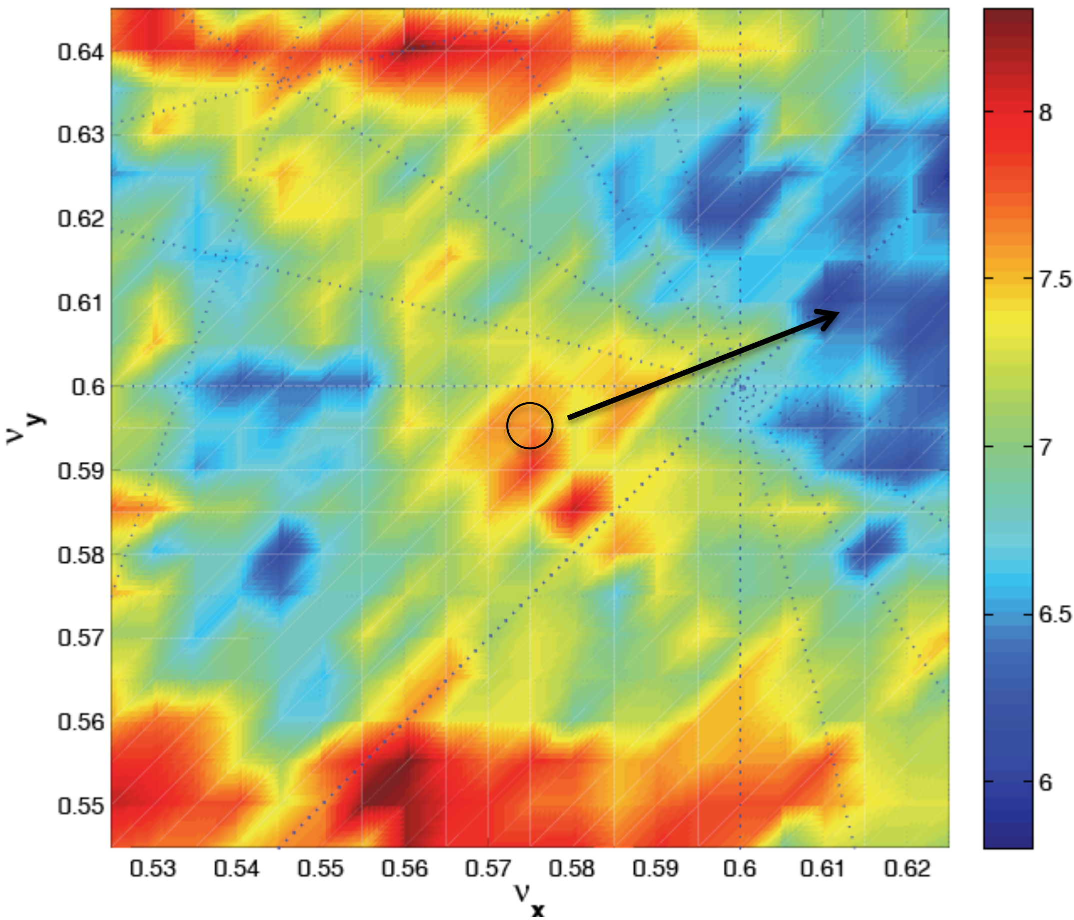

$$WPS = 0.1 N_{lost} + \sum e^D$$

Variable	Symbol	Value
Beam energy	E	7 TeV
Particle species	$\cdots$	protons
Full crossing angle	θ_c	300 μrad
rms beam divergence	σ'_x	31.7 μrad
rms beam size	σ_x	15.9 μm
Normalized transv. rms emittance	$\gamma\varepsilon$	3.75 μm
IP beta function	β^*	0.5 m
Bunch charge	N_b	$(1\times10^{11}-2\times10^{12})$
Betatron tune	Q_0	0.31

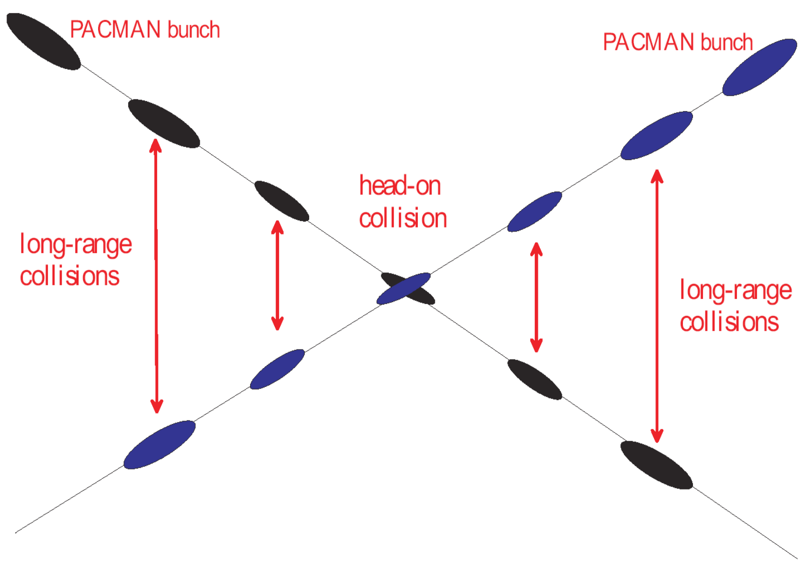

- Long range beam-beam interaction represented by a 4D kick-map

$$\Delta x = -\, n_{par}\,\frac{2r_pN_b}{\gamma}\left[\frac{x'+\theta_c}{\theta_t^2}\left(1-e^{-\frac{\theta_t^2}{2\theta_{x,y}^2}}\right) - \frac{1}{\theta_c}\left(1-e^{-\frac{\theta_c^2}{2\theta_{x,y}^2}}\right)\right]$$

$$\Delta y = -\, n_{par}\,\frac{2r_pN_b}{\gamma}\,\frac{y'}{\theta_t^2}\left(1-e^{-\frac{\theta_t^2}{2\theta_{x,y}^2}}\right)$$

with $\qquad \theta_t \equiv \left((x'+\theta_c)^2+{y'}^2\right)^{1/2}$

Head-on vs Long range interaction

YP and F. Zimmermann, PRSTAB 1999, 2002

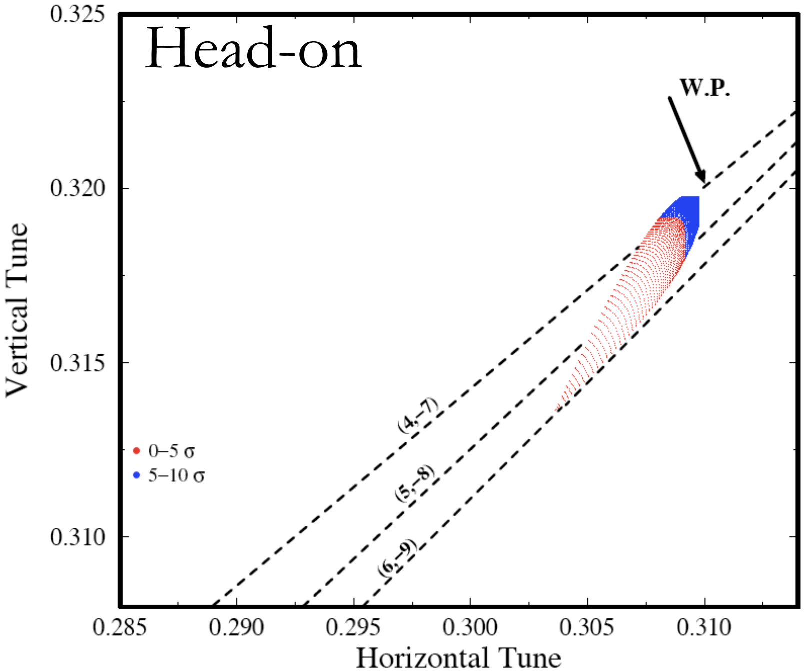

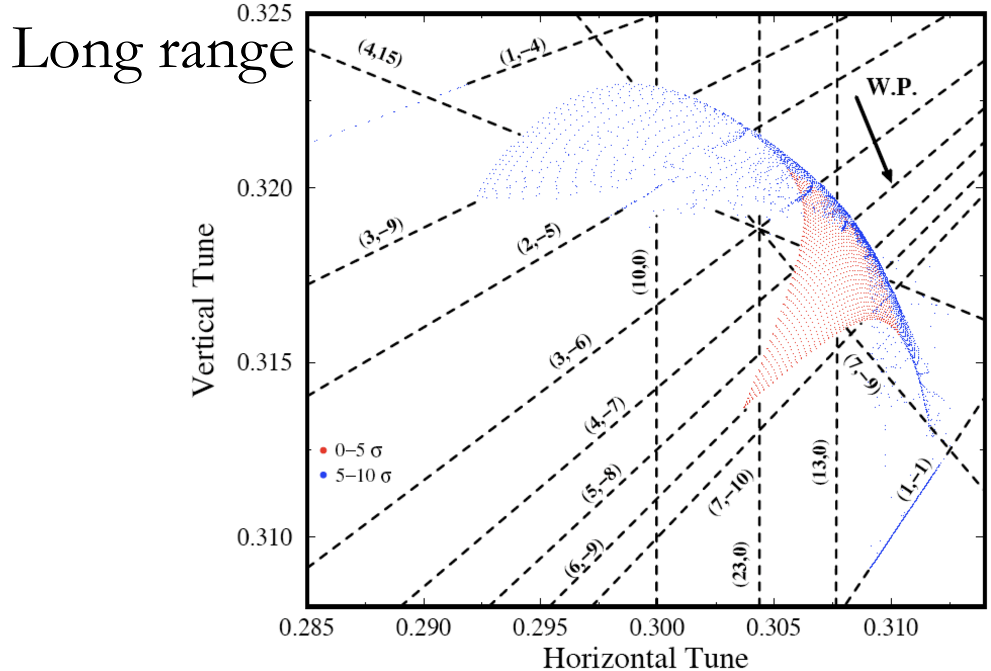

- Proved dominant effect of long range beam-beam effect
- Dynamic Aperture (around 6σ) located at the folding of the map (indefinite torsion)
- Dynamics dominated by the 1/r part of the force, reproduced by electrical wire, which was proposed for correcting the effect
- Experimental verification in SPS and installation to the LHC IPs

Contents of the 2nd lecture

- Resonances and the path to chaos
  - Topology of 3rd and 4th order resonance
  - Path to chaos and resonance overlap
  - Dynamic aperture simulations
- Frequency map analysis
  - NAFF algorithm
  - Aspects of frequency maps
  - Frequency and diffusion maps for the LHC
  - Frequency map for lepton rings
  - Working point choice
  - Beam-beam effect
- Experiments
  - Experimental frequency maps
  - Beam loss frequency maps
  - Space-charge frequency scan

Experimental frequency maps

D. Robin, C. Steier, J. Laskar, and L. Nadolski, PRL 2000

- Frequency analysis of turn-by-turn data of beam oscillations produced by a fast kicker magnet and recorded on a Beam Position Monitors
- Reproduction of the non-linear model of the Advanced Light Source storage ring and working point optimization for increasing beam lifetime

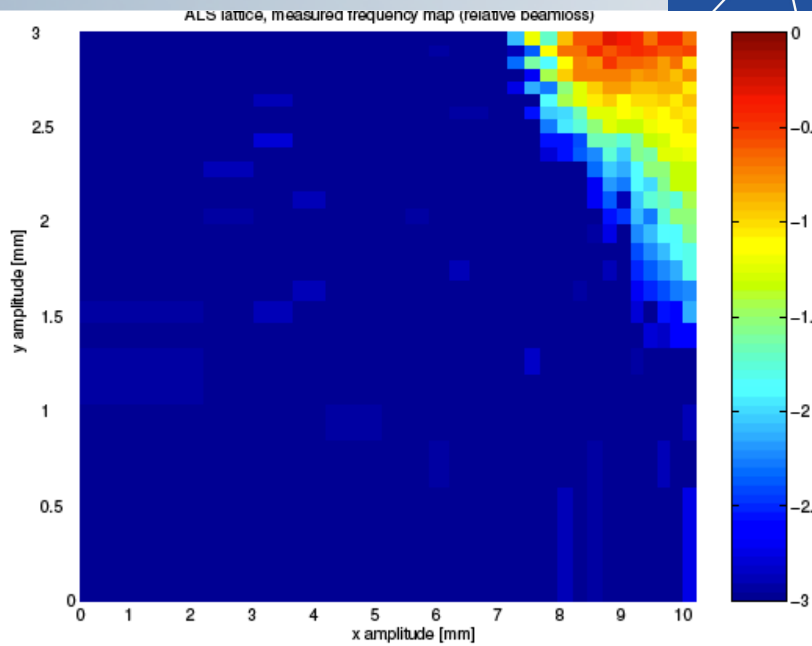

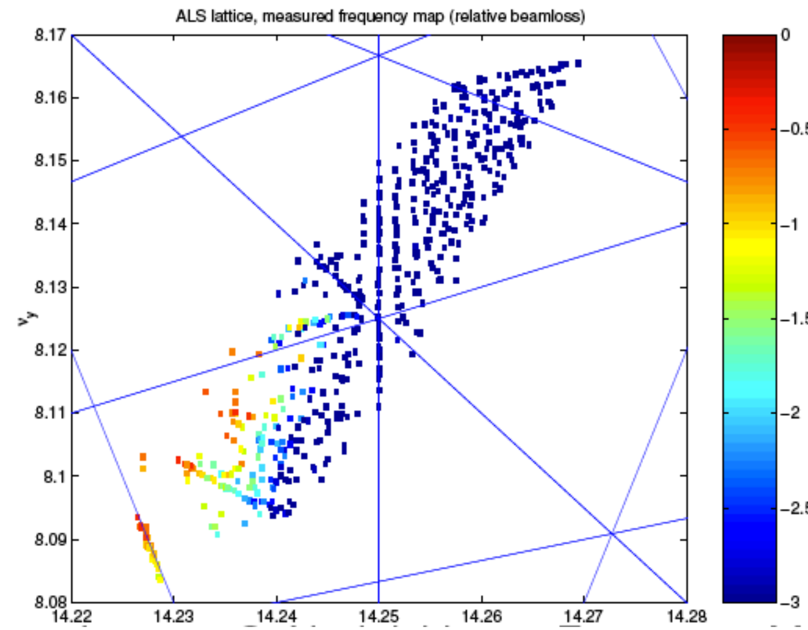

Experimental Methods – Tune scans

- Study the resonance behavior around different working points in SPS
- Strength of individual resonance lines can be identified from the beam loss rate, i.e. the derivative of the beam intensity at the moment of crossing the resonance
- Vertical tune is scanned from about 0.45 down to 0.05 during a period of 3s along the flat bottom
- Low intensity 4-5e10 p/b single bunches with small emittance injected
- Horizontal tune is constant during the same period
- Tunes are continuously monitored using tune monitor (tune post-processed with NAFF) and the beam intensity is recorded with a beam current transformer

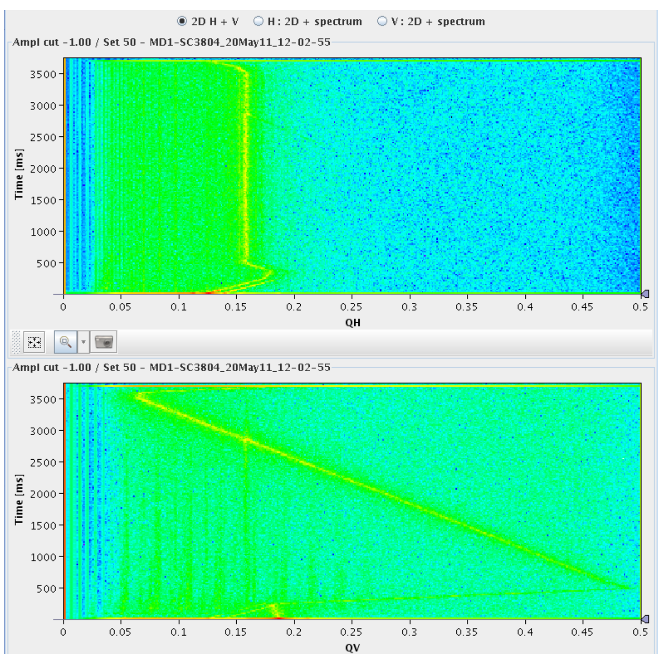

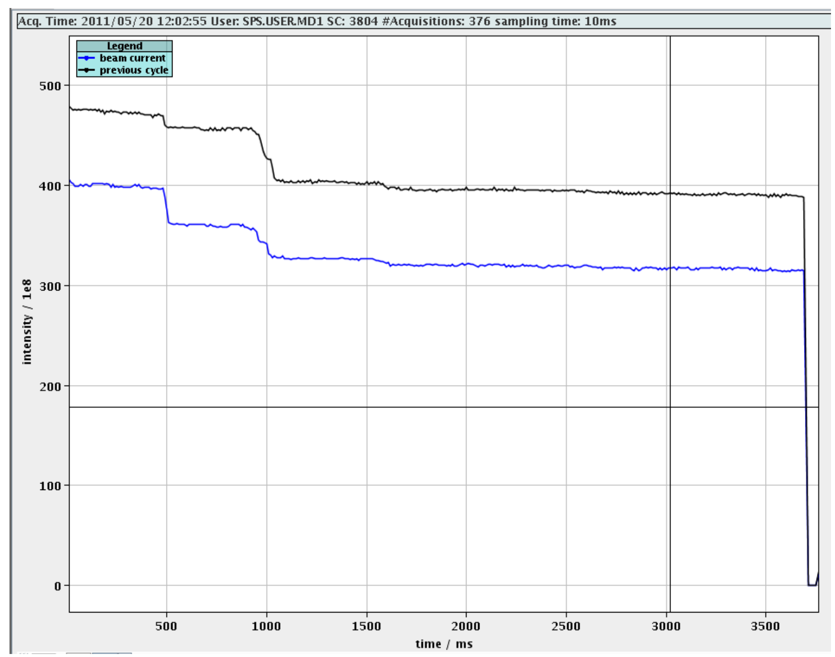

Tune Scans – Results from the SPS

- Resonances in low γ_t optics
  - Normal sextupole Qx+2Qy is the strongest
  - Skew sextupole 2Qx+Qy quite strong
  - Normal sextupole Qx-2Qy, skew sextupole at 3Qy and 2Qx+2Qy fourth order visible

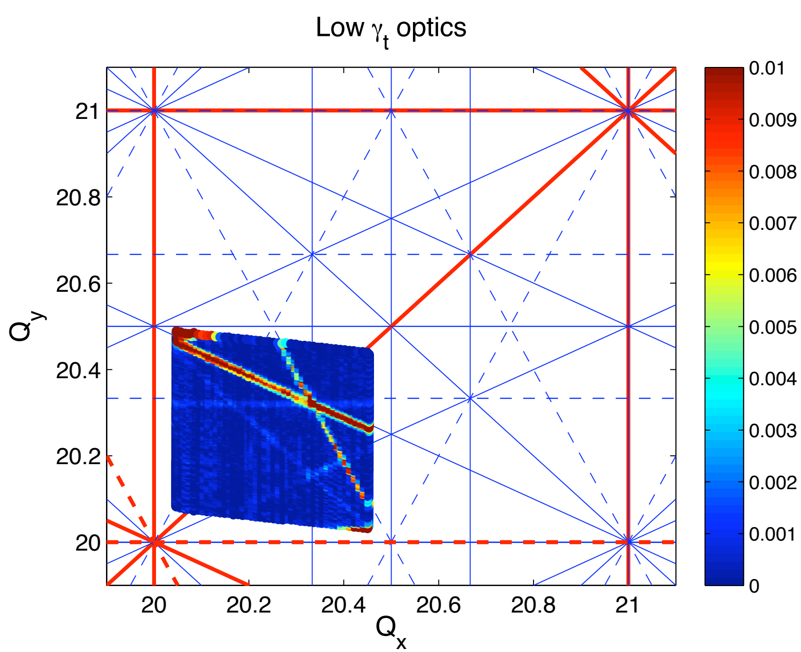

- Resonances in the nominal optics
  - Normal sextupole resonance Qx+2Qy is the strongest
  - Coupling resonance (diagonal, either Qx-Qy or some higher order of this), Qx-2Qy normal sextupole
  - Skew sextupole resonance 2Qx+Qy weak compared to Q20 case
  - Stop-band width of the vertical integer is stronger (predicted by simulations)

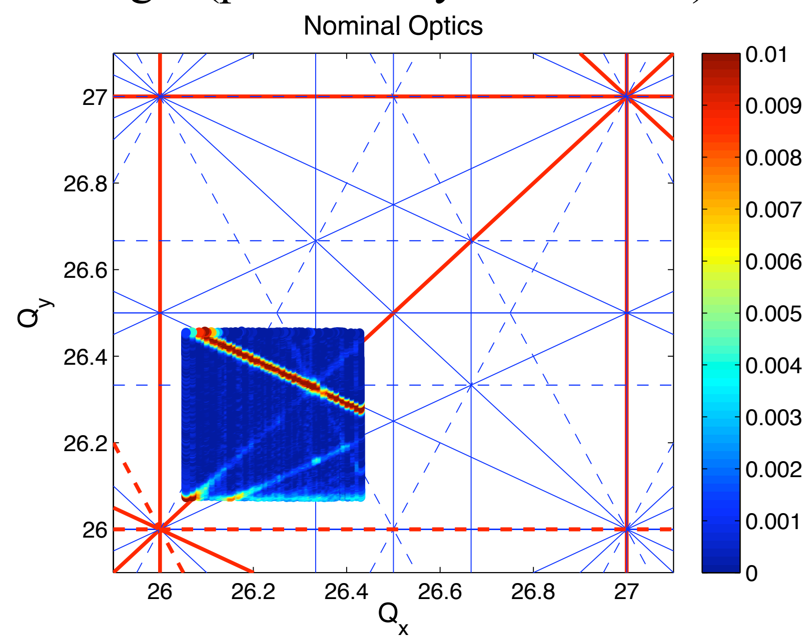

Summary

- Appearance of fixed points (periodic orbits) determine topology of the phase space
- Perturbation of unstable (hyperbolic points) opens the path to chaotic motion
- Resonance can overlap enabling the rapid diffusion of orbits
- Need numerical integration for understanding impact of non-linear effects on particle motion (dynamic aperture)
- Frequency map analysis is a powerful technique for analyzing particle motion in simulations but also in real accelerator experiments

Problems

1) A ring has super-periodicity of 4. Find a relationship for the integer tune that avoids systematic 3rd and 4th order resonances. Generalize this for any super-periodicity.
2) Compute the tune-spread at leading order in perturbation theory for a periodic octupole perturbation in one plane.
3) Extend the previous approach to a general multi-pole.
4) Do skew multi-poles provide 1st order tune-shift with amplitude?